

**GEOCHEMICAL INVESTIGATION OF BASALTS FROM TROIS
MENESTRELS, KERGUELEN ARCHIPELAGO**

by

HABIB EL HADJI SY DIOP

B.S., UNIVERSITÉ CHEIKH ANTA DIOP DE DAKAR, 2000

A THESIS

submitted in partial fulfillment of the requirements for the degree

MASTER OF SCIENCE

Department of Geology
College of Art and Sciences

KANSAS STATE UNIVERSITY
Manhattan, Kansas

2008

Approved by:

Major Professor

KIRSTEN NICOLAYSEN

ABSTRACT

The Kerguelen Archipelago and the submarine Northern Kerguelen Plateau consist primarily of basalt erupted by the intraplate Kerguelen hotspot. The exposed volcanic rocks are tholeiitic basalts (29 Ma) followed by lesser alkalic basalts, highly alkaline phonolites, and syenites (24 Ma). This study presents the mineralogy, isotopic and geochemical compositions of lavas (n=59) from a 650 m section exposed in the wall of a glacial valley at Trois Menestrels in the Kerguelen Archipelago. This basalt section, exposed south of the Cook Ice Cap and closest to the Raillier du Baty alkalic plutonic complex, is further south and west of previously studied basalts exposed on the Plateau Central. Results of $^{40}\text{Ar}/^{39}\text{Ar}$ dating show the Trois Menestrels lavas erupted approximately 25 Ma, approximately contemporaneously with other Plateau Central lavas and thus provide an opportunity to examine spatial compositional variations within the Kerguelen hotspot.

Though the Trois Menestrels lavas are tholeiitic, The samples plot on the tholeiitic field at the stratigraphic section of Trois Menestrels, 80% of lavas from Mt. Tourmente are transitional to alkalic in the younger rocks (25.6 Ma). This sequence of tholeiitic to transitional to alkalic compositions is mirrored at Mt. Capitole and Mt. Marion Dufresne. Sr, Ba, Pb, Nb, Zr versus Nb plots show similar patterns across the Plateau Central and abundances overlap within error. Variations in isotopic composition reveal that Trois Menestrels is rather homogeneous compared to the other sections. A fundamental issue that derives from these results is the close relationship between these different rocks of the various region of the Plateau Central.

Table of Contents

List of Figures	iv
List of Tables	vi
Acknowledgements	vii
Dedication	viii
CHAPTER 1 - INTRODUCTION	1
CHAPTER 2 - BACKGROUND GEOLOGY	5
CHAPTER 3 - ANALYTICAL METHODS	6
CHAPTER 4 - RESULTS SECTION.....	14
Petrography	14
Major elements geochemistry	15
Trace element geochemistry	27
Isotopic composition.....	36
Comparison with other parts of the Kerguelen Plateau Central	37
CHAPTER 5 - DISCUSSION	46
CHAPTER 6 - CONCLUSION	48
CHAPTER 7 - REFERENCES CITED	49

List of Figures

- Figure 1. Location of Kerguelen Archipelago in Indian Ocean compiled using Geomapapp an application that compiles images using satellite gravity data and multibeam bathymetry (www.geomapapp.org; www.marine-geo.org; Carbotte et al., 2004). The Kerguelen Province includes the Kerguelen Plateau and Archipelago plus Broken Ridge and Ninetyeast Ridge. Shallow areas are brown or red in color. SEIR= Southeast Indian Ridge; SWIR= Southwest Indian Ridge; CIR= Central Indian Ridge; RTJ= Rodriguez Triple Junction..... 3
- Figure 2. Map of Kerguelen Archipelago showing locations of sampled stratigraphic sections. Eruption ages are indicated within parentheses. Green dot represents study area. Blue dots represent previous studied sections from the Plateau Central..... 4
- Figure 3 Simplified map of the Plateau Central region of the Kerguelen Archipelago (Google Earth). The Plateau Central (>1100 km²) is dominantly covered by flood basalts that dip 5° to the southeast, and is bordered to the west by the Cook Ice Cap. 8
- Figure 4. Photos showing the 650 m stratigraphic section of lavas exposed at Mt. Trois Menestrels. 9
- Figure 5. Photomicrographs of plagioclase sparsely phyric basalts. Note the existence of olivine-pyroxene plagioclase aggregate in K2M-18 (a) and an aggregate of single plagioclase crystals in K2M-19 (b)..... 10
- Figure 6. Microphotograph of a plagioclase in sparsely phyric (a K2M-52) and close to aphyric (b K2M-7) lavas. The field of view (FOV) is 5.5 mm width for each image. 11
- Figure 7. Total alkali vs. silica classification diagram of Le Maitre et al. (1989) with the tholeiitic-alkaline boundary from Irvine-Baragar (1971). Nearly all of the Trois Menestrels samples cluster under the tholeiitic-alkalic boundary line. K2M-12 and K2M-57 are the most alkalic and plot right above the line. Compositions of Trois Menestrels lavas are subalkalic tholeiitic basalts..... 17

Figure 8. Major elements (all in wt. %) vs. Mg# and vs Silica. All samples define a negative trend for TiO ₂ -Mg# and P ₂ O ₅ -Mg# consistent with control of lava compositions by apatite and Fe-Ti oxide fractionation (see also Fig. 5). But there is considerable scatter with no distinction between Al ₂ O ₃ and CaO plots vs. Mg#.	22
Figure 9. Total alkalis vs. SiO ₂ classification diagram showing the Plateau Central of the Kerguelen Archipelago (classification boundaries from Le Maitre et al., 1989 and Irvine and Baragar, 1971). Sample compositions from Trois Menestrels are blue diamonds. The ~26-25 Ma Mt. Tourmente (Frey et al., 2002), Capitole (Xu et al., 2007), Marion Dufresne (Anell et al., 2006) and Crozier (Frey et al., 2002) basalts are plotted in comparison. The Mt. Tourmente, Capitole and most Marion Dufresne basalts closely overlap with measured compositions at Mt. Les Trois Menestrels and straddle the alkalic-tholeiitic boundary.....	26
Figure 10 Cr and Ni abundance in (ppm) vs. Mg# in Mt. Les Trois Menestrels.....	29
Figure 11. Incompatible element abundances in selected samples from Mt. Les Trois Menestrels Basalts normalized to primitive mantle estimates of Sun & McDonough (1989).....	30
Figure 12. Fe ₂ O ₃ , K ₂ O, Al ₂ O ₃ /CaO and Na ₂ O vs. SiO ₂ diagrams (all oxides in wt. %) for Mt. Les Trois Menestrels, Tourmente, Capitole and Marion Dufresne.....	31
Figure 13. Abundances of Ce, Y, Zr, U, Ba and Th vs. Nb content (all in ppm).	33
Figure 14. Stratigraphic distribution of Cr, Ca/K and Sr/Rb in the Mt. Les Trois Menestrels sections.	42
Figure 15. (⁸⁷ Sr/ ⁸⁶ Sr) vs. (¹⁴³ Nd/ ¹⁴⁴ Nd) from the Kerguelen Archipelago.....	43
Figure 16. ²⁰⁸ Pb/ ²⁰⁴ Pb vs. ²⁰⁶ Pb/ ²⁰⁴ Pb data from Mt. LesTrois Menestrels and fields for various sections of the Kerguelen Archipelago.	44
Figure 17. Epsilon _{Nd} vs. Epsilon _{Hf} in the Kerguelen Archipelago.....	45

List of Tables

Table 1. Modal mineralogy and petrographic characteristics of Mt. Les Trois Menestrels	7
Table 2. Major (wt. %) and trace element abundances (ppm) for Mt. Les Trois Menestrels basaltic rocks.....	18
Table 3 Sr, Nd, Hf and Pb isotopic data of Mt. Les Trois Menestrels.....	38

Acknowledgements

I would like to thank the department of Geology at K-State for the opportunity of having a Master's in Geology. I am thankful to my committee for its expertise. This research would not be possible without the field efforts in the Kerguelen Archipelago of my academic advisor Dr. Kirsten Nicolaysen and her thorough review of the paper. A special thanks to Dr. Mary Hubbard for her tireless support and constructive comments and criticisms on a first draft of the manuscript. Comments from Dr. Robert Cullers and Dr. Sam Chaudhri have largely clarified and improved this paper. I would also like to thank Dr. Matthew Totten and Dr. Jack Oviatt for their advice and encouragement. I am grateful to Dr. Dominique Weis and Dr. James Scoates for trace element and isotope data acquisition at the Pacific Centre for Isotopes and Geochemical Research at the University of British Columbia and for welcoming me in their house in Vancouver during the summer of 2006. The University of Massachusetts (Amherst) is especially acknowledged for major element analyses by mass spectrometry.

This work has been supported by in part by a National Science Foundation Grant to K. Nicolaysen and by the Department of Geology at K-State.

Dedication

This manuscript is dedicated to my wonderful big family and friends; I am not forgetting Mame Fatou Diame and Professor Ababacar Ly.

CHAPTER 1 - INTRODUCTION

The Indian Ocean contains one of the most complete records of hotspot volcanism, and the origin of these features – the Kerguelen Plateau, Broken Ridge, Ninetyeast Ridge and the Kerguelen Archipelago (Fig. 1) – can be best explained by periodic eruptions from a mantle plume over the last 119 million years, starting shortly after the breakup of Gondwana (e.g., Mahoney et al., 1983, Weis and Frey, 1991; Frey and Weis, 1995; Mahoney et al., 1995; Frey et al., 2000a; Duncan, 2002). However, sampling of this, the second largest oceanic hotspot province, is relatively sparse, and thus it is difficult to investigate the degree to which the Kerguelen plume is chemically heterogeneous at one particular time. Characterization of the elemental and isotopic compositions of magmas produced by a hotspot has been particularly fruitful for constraining the history of and processes within the underlying mantle. Comparison of contemporaneously-erupted, stratigraphically sampled sections of basalt, exposed in glacial valleys on the Kerguelen Archipelago, provides the best opportunity to characterize the heterogeneity of the Kerguelen plume.

Previous studies have documented a shift from largely tholeiitic basalt eruption in the northern archipelago (29-28 Ma) to young, highly alkalic lavas and shallow intrusions (~100 ka to ~10 Ma) (e.g., LaMeyre et al., 1976; Weis & Giret, 1994; Weis et al., 1998; Yang et al., 1998; Nicolaysen et al., 2000; Doucet et al., 2002). Isotopic compositions and trace element ratios of the northern archipelago basalts have been interpreted to indicate be characterized by the presence of a depleted asthenospheric or lithospheric component (i.e. low Sr, Pb and high Hf, Nd isotopic compositions). This isotopic heterogeneity has been ascribed to interaction between Kerguelen mantle plume-derived melts and the Southeast Indian Ridge (SEIR) asthenosphere

(Storey et al., 1988; Gautier et al., 1990; Doucet et al., 2002; Weis and Frey, 2002) that occurred when the migrating ridge was near the plume (Fig. 1) although there has been debate about the details of this interpretation (Yang et al., 1998).

The present study examines the relationship between geographic location, major and trace element compositions, age and isotopic compositions of the basaltic rocks exposed on the Plateau Central of the archipelago. By discussing the results of the geochemical and isotopic compositions as well as $^{40}\text{Ar}/^{39}\text{Ar}$ ages in a 650 m succession of lavas from Mt Les Trois Menestrels (Fig. 2), this study shows that the Kerguelen hotspot was compositionally homogenous at approximately 25 Ma over a distance of 24135m. This contrasts significantly with the documentation of compositional and particularly isotopic heterogeneity when the entire 119 million year output of the Kerguelen hotspot is considered.

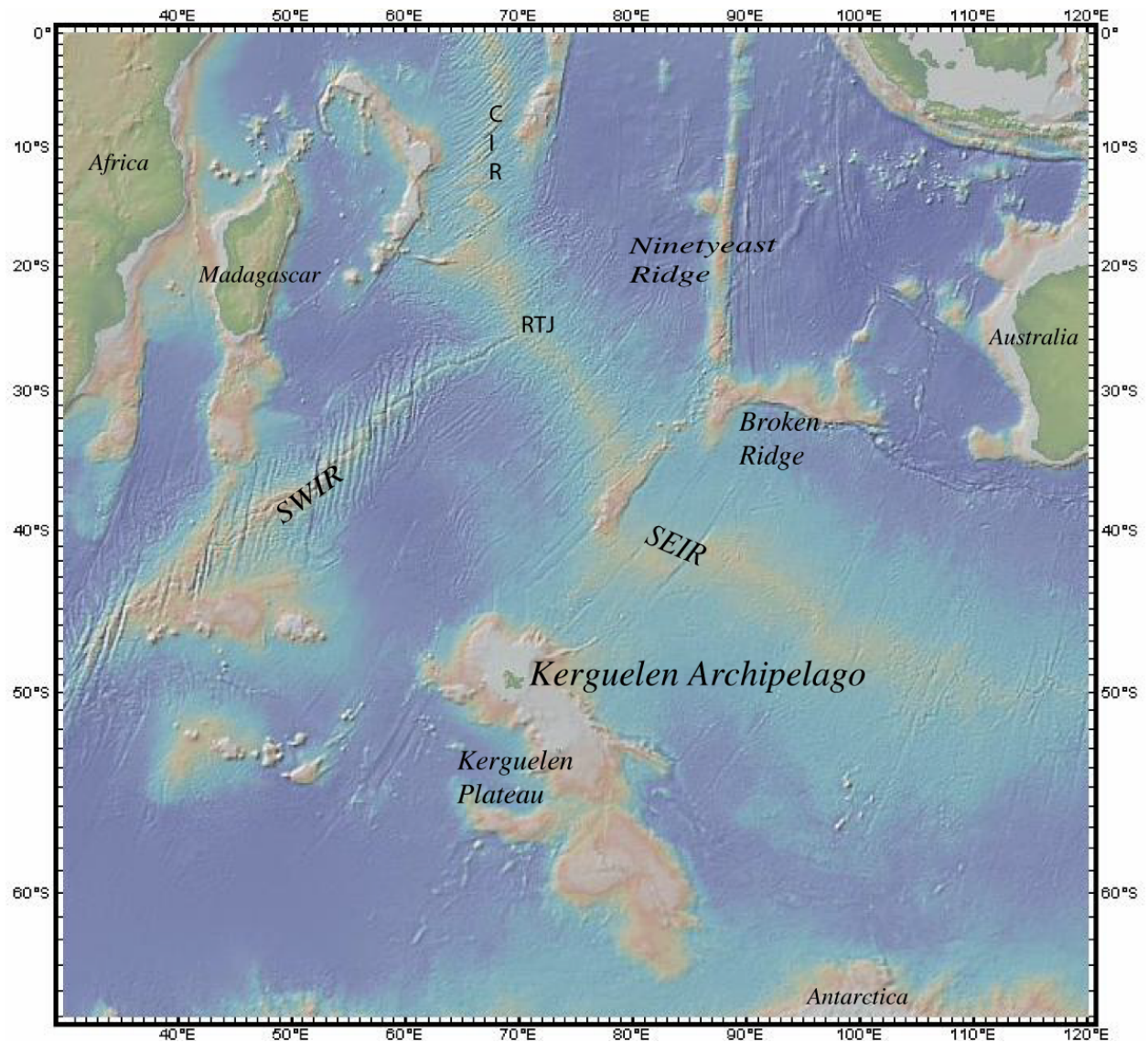


Figure 1. Location of Kerguelen Archipelago in Indian Ocean compiled using Geomapapp an application that compiles images using satellite gravity data and multibeam bathymetry (www.geomapapp.org; www.marine-geo.org; Carbotte et al., 2004). The Kerguelen Province includes the Kerguelen Plateau and Archipelago plus Broken Ridge and Ninetyeast Ridge. Shallow areas are brown or red in color. SEIR= Southeast Indian Ridge; SWIR= Southwest Indian Ridge; CIR= Central Indian Ridge; RTJ= Rodriguez Triple Junction.

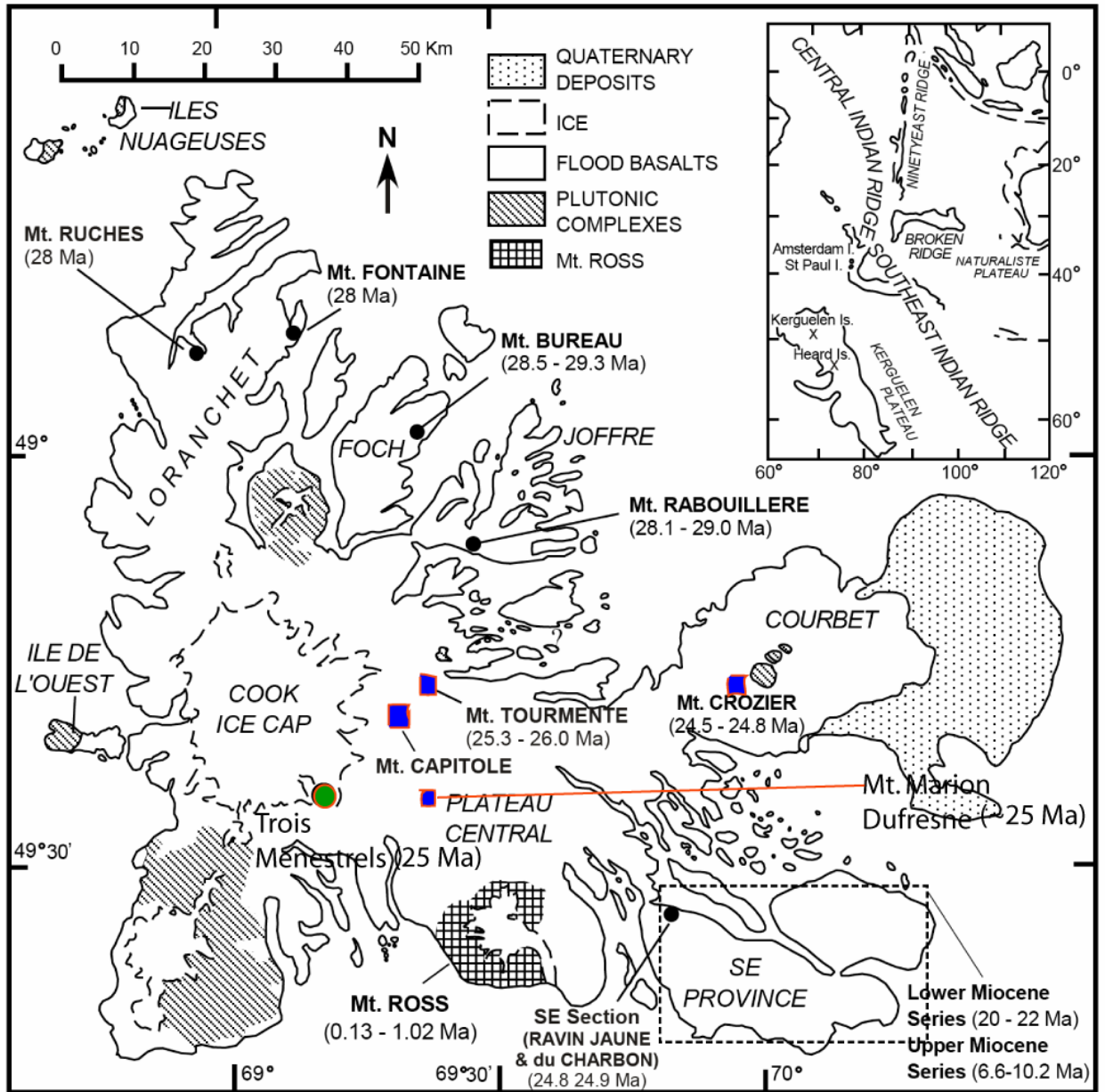


Figure 2. Map of Kerguelen Archipelago showing locations of sampled stratigraphic sections. Eruption ages are indicated within parentheses. Green dot represents study area. Blue dots represent previously studied sections from the Plateau Central.

CHAPTER 2 - BACKGROUND GEOLOGY

Geologic Setting

Widespread Cretaceous and Cenozoic basaltic volcanism in the Indian Ocean has been related to the activity of the Kerguelen mantle plume (e.g., Duncan, 1978; Mahoney et al., 1983; Davies et al., 1989). Changing motions of the Antarctic, Australian, and Indian plates have dispersed these igneous provinces from their original sites of emplacement (Müller et al., 1993). In the larger context of the Indian Ocean volcanic and tectonic evolution, the 120 Ma Kerguelen Plateau (2 million km²) is the oldest oceanic portion of the Kerguelen hotspot-mantle plume system, which later formed the Ninetyeast Ridge, Broken Ridge and the Kerguelen Archipelago (Fig. 1).

The Kerguelen Archipelago is a large oceanic island located approximately S 49°, E 70° in the southern Indian Ocean. It comprises a central island of 100 km width with > 300 smaller islands scattered around the main island (Fig. 2). With a total surface area of over 6500 km², it is the third largest oceanic island after Iceland and Hawaii. The Kerguelen Archipelago is the emergent part of the Northern Kerguelen Plateau, which is an oceanic plateau up to 20-25 km thick (Recq et al., 1994; Charvis et al., 1995; Charvis & Operto, 1999). The Kerguelen Plateau, the second largest oceanic plateau after the Ontong-Java Plateau in the western Pacific Ocean, is attributed to hotspot volcanism from the deep-seated Kerguelen mantle plume (e.g., Mattielli et al., 2002).

The exposed flood basalts (29-24 Ma) cover ~85% of the surface area of the Kerguelen Archipelago (Fig. 2), and comprise older tholeiitic-transitional lavas in the Northern part of the archipelago, and increasingly younger and more alkalic lavas in the Plateau Central region (~26

Ma) and eastern parts of the archipelago (25-24 Ma). The remaining area is occupied by sedimentary deposits (~10%) and intrusive rocks (~5%). These intrusive rocks span a wide compositional range and include alkalic plutonic complexes (Railler du Baty and Société de Géographie) and smaller gabbroic intrusions (Val Gabbro and Montagnes Vertes) exposed by erosion (Giret, 1983; Giret & Lameyre, 1983; Weis & Giret, 1994; Scoates et al., 2007).

Mt. Les Trois Menestrels is located at approximately S 49°26', E 69°07' near the southern edge of the Cook Ice Cap (Fig. 3). Glaciation has exposed a 650 m vertical section of subaerially erupted lava flows cut by one near-surface basaltic sill and two dikes (Fig. 4). From this section, we obtained 59 samples of which all were examined petrographically. I selected 21 samples for analysis of their major and trace element abundances and isotopic compositions.

CHAPTER 3 - ANALYTICAL METHODS

Fifty-nine samples from distinct basaltic rocks were examined, of which fifty-six are aphyric (<5 vol. % phenocrysts, Table 1).

A systematic estimate of the proportion (mode) of the total plagioclase crystals was undertaken using Adobe Photoshop software. This program constitutes powerful tools that help quantify the percentage more easily than the traditional counting method and saves time by automating common tasks. I analyzed 177 photomicrographs, that is to say I took three digital photographs of each thin section for all 59 samples (in order to have a good representation of each part of the entire section). Characterization consisted of taking the ratio of plagioclase pixels (gray and white pixels identified by the software) to all pixels present in the image; for the Fe-Ti oxides I calculated the ratio of black pixels in plane polarized light to all pixels. The crystal abundances were characterized using the petrographic microscope in both plane and

Table 1. Modal mineralogy and petrographic characteristics of Mt. Les Trois Menestrels

Sample	Altitude (m)	Rock name	Mineral abundances (vol. %)				Plagioclase phenocryst size (mm)	Plagioclase zonation	Special features	Unit	Calcite	Dike/Sill
			Plag	Cpx	Ol	Fe-Ti ox						
K2M-1	19	Thol. Basalt	17.16	5-6	-	47	0.02-1.5 mm		holocrystalline	A	-	-
K2M-2	25	Thol. Basalt	27.28	10	-	26	0.02-2.3 mm			A	-	-
K2M-3	37	Thol. Basalt	13.49	6	2-3	50				A	-	-
K2M-4	50	Thol. Basalt	4-5	1-2	0-1	biased				A	+	-
K2M-5	60	Thol. Basalt	5	1-2	-	25				A	-	-
K2M-6	85	Thol. Basalt	3.62	2-3	-	18	0.02-1.5mm,	NZ		A	-	-
K2M-7	87	Thol. Basalt	4.73	3	-	33	0.03-2mm		tiling	A	-	-
K2M-8	91	Thol. Basalt	29.9	9	2-3	17	0.02-2mm			A	-	-
K2M-9	109	Thol. Basalt	12.85	3	-	47	0.02-2mm			A	-	-
K2M-10	121	Thol. Basalt	17.39	3	-	49	<0.02-0.5mm			A	+	-
K2M-11	135	Thol. Basalt	19.36	6	-	30	0.02-1.2mm		holocrystalline	A	-	-
K2M-12	158	Thol. Basalt	17.42	2	-	35	2Pop			A	-	-
K2M-13	180	Thol. Basalt	16.57	2	-	23	2Pop, incl.			A	-	-
K2M-14	185	Thol. Basalt	11.73	1-2	-	25				A	-	-
K2M-15	205	Thol. Basalt	21	3	-	32				A	-	-
K2M-16	220	Thol. Basalt	17	3	-	21				A	+	-
K2M-17	230	Thol. Basalt	19	4	-	19				A	-	-
K2M-18	245	Thol. Basalt	26	3	1	18	2Pop			A	-	-
K2M-19	255	Thol. Basalt	26	5	-	20	0.02-2mm			A	-	-
K2M-20	259	Thol. Basalt	2-4	2	-	20				A	-	-
K2M-21	262	Thol. Basalt	13	4	-	33			glomerocrysts	A	-	-
K2M-22	267	Thol. Basalt	5	3	-	39				A	-	+
K2M-23		Thol. Basalt	9	4	-	55				A	-	-
K2M-24	278	Thol. Basalt	9	3	-	42				A	-	-
K2M-25		Thol. Basalt	18	3	-	34				A	-	-
K2M-26	298	Thol. Basalt	18	5	-	50	2P 0.02-2mm,	NZ		A	-	-
K2M-27	310	Thol. Basalt	27	4	-	15				A	-	-
K2M-28	318	Thol. Basalt	17.5	4	-	21	1-2mm,	NZ		A	-	-
K2M-29	323	Thol. Basalt	22	4	-	18				A	-	+
K2M-30	328	Thol. Basalt	11	4	-	56				B	-	-
K2M-31		Thol. Basalt	8	6	-	32			holocrystalline	B	-	-
L2M-32		Thol. Basalt	18	7	-	29			holocrystalline	B	-	-
K2M-33	358	Thol. Basalt	22	6	-	31	2Pop,	NZ	holocrystalline	B	-	-
K2M-34		Thol. Basalt	3-4	3	-	41				B	+	-
K2M-35	368	Thol. Basalt	17	4	-	35				B	-	-
K2M-36	380	Thol. Basalt	12	3	-	16				B	-	-
K2M-37	385	Thol. Basalt	6.4	5	-	21			holocrystalline	B	-	-
K2M-38		Thol. Basalt	24	7	-	13				C	-	-
K2M-39		Thol. Basalt	21	4	-	10				C	-	-
K2M-40		Thol. Basalt	21	2	-	15				C	-	-
K2M-41	480	Thol. Basalt	33	3	-	14				C	-	-
K2M-42		Thol. Basalt	26	6	-	26				C	-	-
K2M-43		Thol. Basalt	28	6	-	28				C	-	-
K2M-44		Thol. Basalt	20	2	-	27				C	-	-
K2M-45		Thol. Basalt	23	4	-	15				C	-	-
K2M-46	510	Thol. Basalt	33	2	-	13				C	-	-
K2M-47	550	Thol. Basalt	21	2	-	29				C	-	-
K2M-48		Thol. Basalt	17	6	-	15				C	-	-
K2M-49	590	Thol. Basalt	25	6	2-3	30				C	-	-
K2M-50	600	Thol. Basalt	25	5	-	28				C	-	-
K2M-51	610	Thol. Basalt	16	2	-	18				C	-	-
K2M-52	625	Thol. Basalt	24	2	-	11				C	-	-
K2M-53		Thol. Basalt	30	2	-	17	0.02-2 mm			C	-	+
K2M-54	650	Thol. Basalt	28	6	-	23	0.02-1.5 mm			C	-	-
K2M-55		Thol. Basalt	2-3	2	-	5			glassy	C	-	-
K2M-56		Thol. Basalt	34	6	-	20				C	-	+
K2M-57		Thol. Basalt	20	4	-	29				C	-	-
K2M-58		Thol. Basalt	31	7	-	15				C	-	-
K2M-59		Thol. Basalt	31	6	-	18				C	-	-

NZ = normal zoning; 2P = 2Pop = two different populations of plagioclase

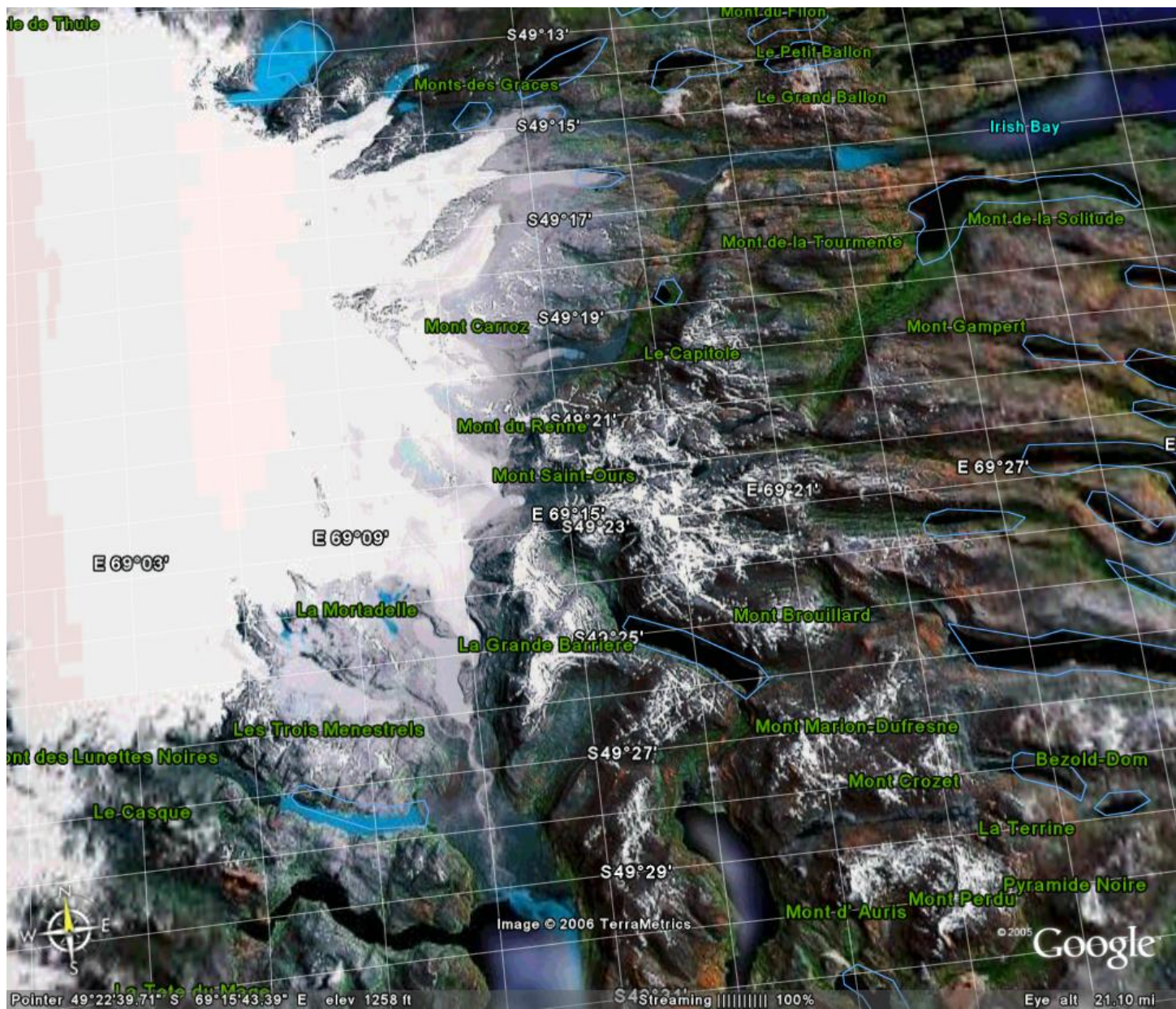
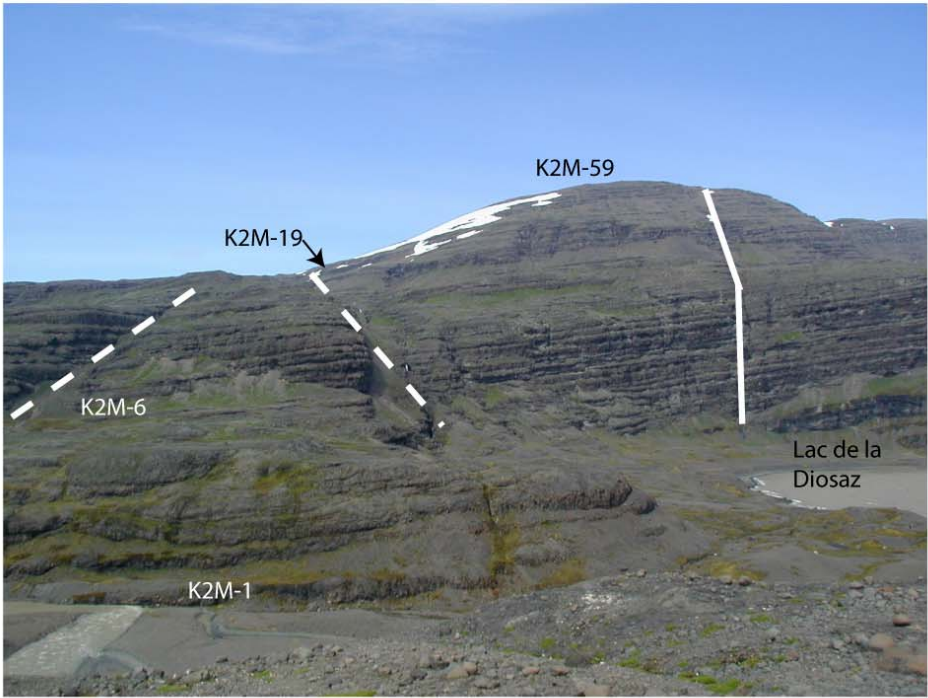


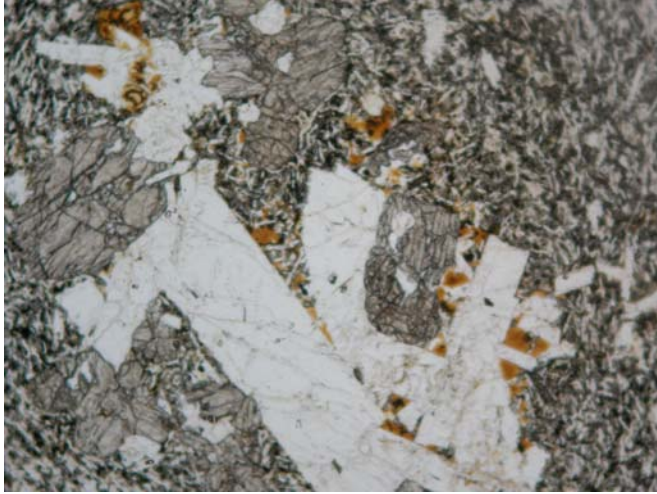
Figure 3 Simplified map of the Plateau Central region of the Kerguelen Archipelago (Google Earth). The Plateau Central (>1100 km²) is dominantly covered by flood basalts that dip 5° to the southeast, and is bordered to the west by the Cook Ice Cap.



a) Antithetic figure. b) View looking South from La Mortadelle at the stratigraphic section of Trois Menestrels.
K2M-1/K2M-59= sample numbers.

 =dike  =faults

Figure 4. Photos showing the 650 m stratigraphic section of lavas exposed at Mt. Trois Menestrels.

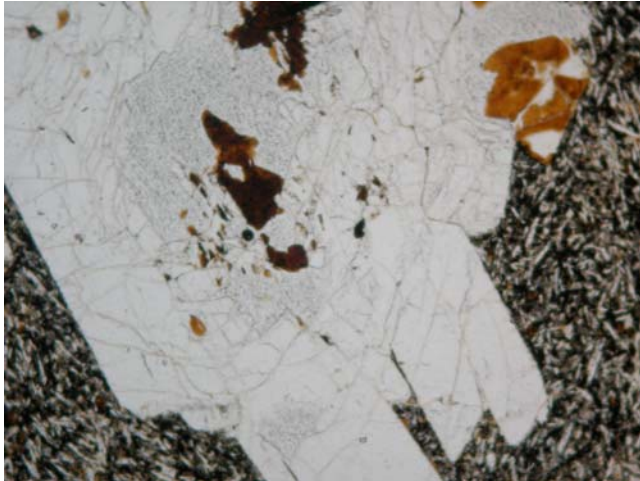


a

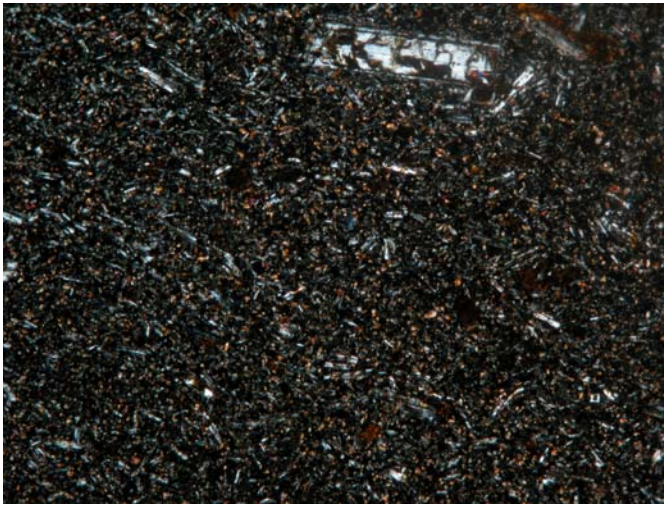


b

Figure 5. Photomicrographs of plagioclase sparse pyritic basalts. Note the existence of olivine-pyroxene plagioclase aggregate in K2M-18 (*a*) and an aggregate of single plagioclase crystals in K2M-19 (*b*).



a



b

Figure 6. Microphotograph of a plagioclase in sparsely phyric (*a* K2M-52) and close to aphyric (*b* K2M-7) lavas. The field of view (FOV) is 5.5 mm width for each image.

cross-polarized lights for titanomagnetite. Olivine and pyroxene represent minor phases that display a range of colors in cross-polarized light, making them difficult to analyze by this technique. The abundances of these phases were approximated visually.

I selected a subset of 21 samples representative of the entire suite (n=59) for the geochemical analyses. These samples were chosen after assessing them petrographically to have minimal amounts of alteration and after prioritizing samples such that the entire stratigraphic sequence was represented. First I crushed the samples coarsely using a hydraulic crusher with hardened tungsten carbide surfaces and then reduced the samples to a fine powder using an agate mortar. Subsequently, major elements and certain trace elements were analyzed by X-ray fluorescence (XRF) at the University of Massachusetts, Amherst (Rhodes, 1996). Other trace elements as well as Nd, Hf, Pb and Sr isotopic analyses were carried out using a Thermo-Finnegan multi-collector inductively-coupled mass spectrometer (MC-ICPMS) at the Pacific Centre for Isotopic and Geochemical Research (PCIGR) at the University of British Columbia in Vancouver. Prior to dissolution, all samples were leached in 6N HCl in an ultrasonic bath to remove secondary minerals following the procedure of Weis & Frey (1996).

Sample preparation for isotopic analysis

To dissolve the powders, 2ml of concentrated sub-boiled HF and 500 micro liters of concentrated Seastar HNO₃ were added. The samples were sealed and placed on a hotplate for 48 hours at a temperature of approximately 120°C. The samples were placed (twice during the 48 hours) in an ultra-sonic bath for 15 minutes to ensure complete dissolution of the powder. The samples were then uncapped and placed on a hotplate until dry. Once dry, 2ml of Seastar concentrated HNO₃ were added. After 24 hours on the hotplate, the samples were uncapped and dry once again. Approximately 4g of a stock solution of 1% HNO₃ spiked with 1 ppb Indium

(In) were added and the samples were placed on a hotplate for 24 hours. The sample were placed (twice during this time interval) in an ultra-sonic bath for 15 minutes to ensure complete redissolution. The samples were then transferred to clean 125 ml high density polyethylene (HDPE) sample bottles. Two separate dilutions were carried out. Samples were diluted to 1000 times for rare earth elements (REE), and 2000 times for all other elements, after an initial dilution to 1000 times their initial weight with stock solution of 1% HNO₃ with 1ppb In. A portion of the 1000 times diluted mixture was transferred to clean 60 ml HDPE sample bottles and subsequently diluted to 2000 times. A proportional amount of concentrated HCl was added to each of the 2000 times dilutions so that the resulting solutions would have a concentration of 1% HCl.

The rare earth elements were measured in high resolution, while Pb and U were measured in low resolution. Most remaining elements were measured in medium resolution mode. A series of 6 standards, obtained by series of dilution from 1000 ppm High Purity stock standard solutions using 1% HNO₃ with 1 ppb In, was used for external calibration and concentration calculation.

Data quality

To evaluate the reproducibility of the results, two duplicate analyses were run. Listed trace element compositions are the mean of duplicate analyses although in that case both analytical duplicates needed to be within acceptable error criteria (Table 2). The precision of the measurements was controlled by replicate measurements. All the elements show reasonable variation for total procedural duplicate, except for Nb, Mo, Sn, Ta, and W, which present a variation for total duplicate greater than 10%. Hf, Zr, Bi, Cr, Sb, which have variation for total duplicate between 5 and 10%. Repeated measurements of a USGS basaltic reference material

(BHVO-2) and an internal standard (1140A-31R-1) were also made to ensure exact concentration results. Procedural blank values were in the parts-per trillion (ppt) range and are considered negligible in comparison to the sample concentrations, which are in parts-per-million (ppm) range. A solution of 4% aqua regia + 0.05 % HF was used to rinse the instrument between each sample to minimize memory effects from previously analyzed sample. Background values were checked periodically during the course of analysis, particularly after high abundance samples or standards, to detect and correct for memory effects. Indium, which is spiked at 1 ppb in all blank, standard, and sample solutions, was used as an internal standard to monitor and correct for sensitivity drift. Low-level (5 ppb) REE standard solutions were run after every fifth or sixth sample to detect and correct for instrumental mass drift.

CHAPTER 4 - RESULTS SECTION

Petrography

The petrographic study of Trois Menestrels basalts shows that the samples are close to aphyric, with the total plagioclase content varying between ~3 to 32% (mainly groundmass microlites). The abundance of phenocrysts is generally <2% by volume and never exceeds 7% by volume, so the basalts range from aphyric to very sparsely phyric. Three samples are sparsely phyric with 5-6 % plagioclase, 2-3 % clinopyroxene, ~1% olivine (K2M-18), 4-5 % plagioclase, ~1 % clinopyroxene (K2M-19) and 6-7 % plagioclase (K2M-52). These samples were taken from the middle and near the top of the section (Figs. 5 & 6). The modal mineralogy of the Trois Menestrels demonstrates the predominance of plagioclase crystals; they show extreme variation in size, typically 0.3-3 mm. The olivine content is typically less than 3% and the microphenocrysts range from 0.03 to 0.3 mm in size. The olivine crystals are partly or

completely altered and are identified by their distinctive crystal form (K2M-10). Olivine occurs in lavas found at the top and at the base of the section.

Clinopyroxene in basaltic units of Trois Menestrels is typically augite and occurs as single crystals, whereas the clinopyroxenes in the dikes and sill are generally subophitic. Vesicles and veins are filled with chlorite (as in K2M-17-20) and calcite. Trois Menestrels basaltic rocks are high iron titanium rich with 15-16 wt. % Fe_2O_3 and 3-4 wt. % TiO_2 ; in most thin sections Fe-Ti oxides are very abundant in the groundmass but do not occur as phenocrysts.

Initial comparison of the basaltic rocks from all Plateau Central studies shows that the spatially disparate lava sections have different characteristics that include the phase proportions. Samples from Trois Menestrels (TM) are aphyric to sparsely phyric. Lavas from Mt. Tourmente, a 500-m-high section located ~24 km northeast of the Trois Menestrels study site, are aphyric. Only two of the 64 samples are plagioclase- and clinopyroxene-phyric (Frey et al., 2002a). Younger flood basalt lavas can be significantly more plagioclase phyric, with mildly alkalic basalts having up to ~17 % plagioclase in lavas from Mt. Crozier, (~ 64 km east from TM; Damasceno et al., 2002). Phase proportions in lavas from the lowermost 300 m of the Marion Dufresne section located 17 km southeast of TM, demonstrate that the lavas are dominantly aphyric but up to 60% plagioclase-phyric in the younger rocks (Annell et al., 2006). The same succession is observed at Mt. Capitole with aphyric lavas in the lower transitional group to plagioclase-phyric in the upper transitional group (Xu et al., 2007).

Major elements geochemistry

Major element classification shows that most of the samples plot in the field of tholeiitic basalt (Fig.7). Samples K2M-12, K2M-57 and K2M-33, K2M-35 plot right above and across the line respectively. The tholeiitic basalts at Mt. Trois Menestrels have a restricted range of

relatively low SiO₂ contents, from 40 to 50 weight percent; nonetheless these are not primary magmas. Mg# ($Mg\# = Mg / (Mg + Fe) = 0.32 - 0.44$) is particularly low suggesting that the parent magmas for the Trois Menestrels fractionated at depth. In general MgO and Fe₂O₃ are negatively correlated with silica suggesting the crystallization of clinopyroxene and olivine. TiO₂ increases with decreasing Mg# (Fig. 8), a trend typically interpreted as evidence that iron-titanium oxides are not yet saturated in the magma and have not crystallized at depth. Al₂O₃ vs Mg# and silica does not show a clear pattern (Figs. 8, 9) suggesting that if crystal fractionation of plagioclase is occurring the mass of plagioclase left at depth is quite small. CaO/Al₂O₃ vs silica (Fig. 9) has essentially no slope supporting the relative unimportance of plagioclase fractionation at depth. Potassium oxide (wt. % K₂O=0.4-1.1) does not show a particularly linear trend with silica and this may indicate some post-crystallization mobilization of alkali due to meteoric or hydrothermal alteration. This will be evaluated in later sections using trace element data.

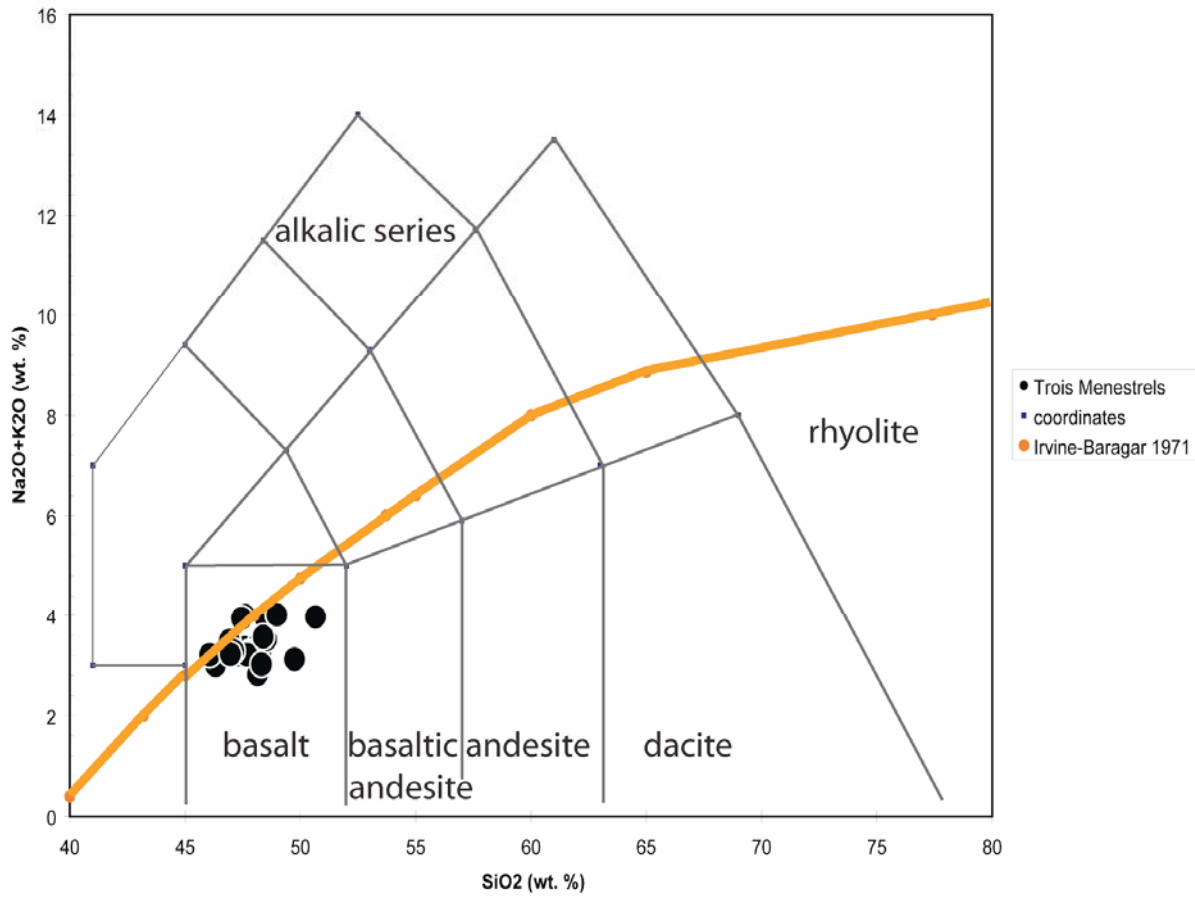


Figure 7. Total alkali vs. silica classification diagram of Le Maitre et al. (1989) with the tholeiitic-alkaline boundary from Irvine-Baragar (1971). Nearly all of the Trois Menestrels samples cluster under the tholeiitic-alkalic boundary line. K2M-12 and K2M-57 are the most alkalic and plot right above the line. Compositions of Trois Menestrels lavas are subalkalic tholeiitic basalts.

Table 2. Major (wt. %) and trace element abundances (ppm) for Mt. Les Trois Menestrels basaltic rocks

Notes: Units on the Majors are wt % and Fe₂O₃ is TOTAL Fe. Totals have **NOT** been resummed using the LOI value

Sample	Relative strat position	SiO ₂	TiO ₂	Al ₂ O ₃	Fe ₂ O ₃ *	MnO	MgO	CaO	Na ₂ O	K ₂ O
K2M-1	1	50.66	3.61	13.36	14.57	0.23	4.56	8.91	3.20	0.77
K2M-3	3	48.46	3.96	13.32	16.07	0.26	4.28	8.98	2.97	0.98
K2M-5	5	48.28	4.18	13.74	15.02	0.24	4.53	9.65	2.60	0.64
K2M-10	10	49.75	3.25	13.40	14.02	0.22	5.60	9.81	2.54	0.58
K2M-12	12	47.59	3.96	14.16	15.30	0.35	5.22	8.96	2.96	1.04
K2M-15	15	47.61	3.66	13.47	15.87	0.31	5.63	9.61	2.91	0.44
K2M-18	18	48.15	3.50	13.98	15.14	0.24	5.40	9.96	2.55	0.27
K2M-20	20	48.21	3.67	13.67	14.91	0.26	5.56	9.94	2.62	0.82
K2M-21	21	47.75	3.67	13.44	15.78	0.24	5.36	9.78	2.59	0.66
K2M-22	22	46.32	4.00	13.67	16.87	0.28	5.09	10.16	2.69	0.31
K2M-25	25	48.54	3.63	13.23	15.56	0.26	4.95	9.53	2.85	0.67
K2M-26	26	47.29	3.86	13.56	15.59	0.22	5.17	10.13	2.53	0.68
K2M-29	29	47.69	3.49	13.76	15.82	0.24	4.93	10.19	2.85	0.36
K2M-33	33	46.06	4.24	13.62	16.57	0.26	5.17	10.25	2.77	0.44
K2M-35	35	46.92	3.92	13.26	16.38	0.24	5.03	10.23	2.85	0.64
K2M-49	49	47.11	3.81	13.58	16.39	0.25	4.80	9.90	2.87	0.41
K2M-50	50	48.31	3.86	13.54	15.72	0.24	5.44	9.71	2.67	0.35
K2M-52	52	46.97	3.84	13.48	16.60	0.28	5.25	10.07	2.81	0.41
K2M-56	56	48.39	4.03	12.95	16.38	0.23	4.14	9.44	2.76	0.81
K2M-57	57	47.45	4.14	13.42	15.80	0.22	4.74	9.39	2.92	1.02
K2M-59	59	48.98	3.93	13.05	15.55	0.25	4.36	9.25	2.92	1.09

Table 2 (cont.)

	P₂O₅	Total	LOI	Na₂O+K₂O	CaO/Al₂O₃	K (ppm)	Mg#
K2M-1	0.46	100.33	0.90	3.97	0.67	3196.11	0.37
K2M-3	0.58	99.86	1.64	3.95	0.67	4067.77	0.34
K2M-5	0.56	99.44	2.40	3.24	0.70	2656.50	0.37
K2M-10	0.36	99.53	0.30	3.12	0.73	2407.46	0.43
K2M-12	0.48	100.02	2.31	4.00	0.63	4316.82	0.40
K2M-15	0.41	99.92	1.30	3.35	0.71	1826.35	0.40
K2M-18	0.41	99.60	1.28	2.82	0.71	1120.71	0.41
K2M-20	0.45	100.11	2.05	3.44	0.73	3403.65	0.42
K2M-21	0.44	99.71	1.06	3.25	0.73	2739.52	0.39
K2M-22	0.49	99.88	2.15	3.00	0.74	1286.74	0.37
K2M-25	0.45	99.67	0.74	3.52	0.72	2781.03	0.38
K2M-26	0.43	99.46	1.16	3.21	0.75	2822.54	0.39
K2M-29	0.40	99.73	2.86	3.21	0.74	1494.28	0.37
K2M-33	0.48	99.86	1.95	3.21	0.75	1826.35	0.37
K2M-35	0.45	99.92	1.50	3.49	0.77	2656.50	0.37
K2M-49	0.48	99.60	1.98	3.28	0.73	1701.82	0.36
K2M-50	0.41	100.25	0.95	3.02	0.72	1452.78	0.40
K2M-52	0.47	100.18	1.73	3.22	0.75	1701.82	0.38
K2M-56	0.49	99.62	2.05	3.57	0.73	3362.14	0.33
K2M-57	0.51	99.61	1.08	3.94	0.70	4233.80	0.37
K2M-59	0.50	99.88	2.01	4.01	0.71	4524.36	0.35

Table 2 (cont.)

Sample	XRF		XRF ICP			XRF		XRF ICP		XRF ICP		XRF	XRF
	Rb	Sr	Cs	Ba	Sc	V	Cr	Co	Ni	Zn	Ga	Y	
K2M-1	8.5	349	0.2	251	29.0	348	42	35.8	34	134.6	25	39.6	
K2M-3	6.8	317	0.0	254	28.2	324	11	35.4	14	158.5	24	46.1	
K2M-5	7.9	388	0.0	304	28.5	381	40	33.7	38	147.5	24	48.9	
K2M-10	12.4	333	0.2	188	28.8	331	105	37.5	50	122.2	22	32.6	
K2M-12	8.3	319	0.1	281	31.1	389	38	41.9	29	151.4	29	41.7	
K2M-15	4.4	320	0.1	169	32.8	411	42	43.9	44	146.5	28	38.6	
K2M-18	1.2	353	0.0	144	29.5	348	46	41.9	40	134.1	24	37.8	
K2M-20	8.9	317	0.0	191	30.9	341	75	42.4	52	142.2	25	37.6	
K2M-21	5.7	338	0.0	212	29.9	361	59	40.6	45	143.6	25	41.7	
K2M-22	0.4	340	0.0	180	29.0	374	39	41.9	32	141.1	25	40.6	
K2M-25	5.5	340	0.1	235	25.9	333	38	39.0	30	133.3	24	37.4	
K2M-26	5.5	334	0.0	193	33.0	344	77	41.8	39	148.1	25	38.0	
K2M-29	1.9	346	0.0	178	31.4	318	25	43.3	28	146.9	25	34.4	
K2M-33	4.8	324	0.0	198	32.1	353	50	43.7	36	149.1	25	37.9	
K2M-35	2.7	335	0.0	199	30.8	394	40	42.6	33	155.6	28	40.8	
K2M-49	1.4	348	0.0	227	28.7	358	26	39.9	26	150.4	25	39.5	
K2M-50	0.9	375	0.0	178	26.4	347	35	40.4	36	135.6	25	35.1	
K2M-52	6.4	332	0.1	211	28.5	356	87	39.1	38	146.6	25	39.2	
K2M-56	7.7	335	0.0	267	28.0	345	21	41.6	27	161.7	25	40.6	
K2M-57	8.8	338	0.0	253	28.7	389	24	36.7	24	138.2	26	43.4	
K2M-59	20.2	329	0.1	269	26.3	333	22	38.2	26	149.3	25	39.9	
ICP precision													
std dev (ppm)			0.001246		0.831935			0.130343		0.653653			
%RSD			0.616848		2.868964			0.364546		0.485638			
Sample	XRF	XRF ICP		ICP									
	Zr	Nb	Hf	Ta	Th	U	Pb	La	Ce	Pr	Nd	Sm	
K2M-1	289	31.6	5.9	0.7	3.0	0.7	1.6	28.4	63.9	8.0	32.8	8.4	
K2M-3	336	37.3	7.2	0.8	3.6	0.8	1.8	32.5	74.0	9.4	38.2	9.6	
K2M-5	343	37.1	7.2	0.3	3.5	0.8	1.9	32.1	73.1	9.1	37.1	9.4	
K2M-10	223	24.5	4.9	0.8	2.2	0.5	1.2	20.8	46.3	5.9	24.8	6.4	
K2M-12	289	31.3	6.2	1.3	3.2	0.7	1.3	26.9	64.6	8.2	34.1	8.8	
K2M-15	248	27.1	5.5	1.2	2.6	0.5	0.8	21.5	51.9	6.8	28.5	7.6	
K2M-18	247	26.7	5.2	0.9	2.4	0.5	1.3	23.9	54.1	6.8	28.5	7.5	
K2M-20	254	28.2	5.5	0.7	2.5	0.5	1.3	23.5	55.3	6.9	28.8	7.5	
K2M-21	254	27.8	5.3	0.8	2.5	0.5	1.3	25.8	54.9	7.1	30.4	7.9	
K2M-22	275	30.3	5.6	1.1	2.7	0.6	1.4	24.2	56.6	7.1	29.9	7.8	
K2M-25	257	27.8	5.2	1.0	2.6	0.5	1.2	22.0	52.0	6.5	27.4	7.1	
K2M-26	245	27.2	5.7	0.7	2.8	0.5	1.3	24.4	53.6	7.0	30.4	8.0	
K2M-29	230	24.6	4.0	0.6	2.7	0.6	1.3	23.4	51.4	6.7	28.5	7.5	
K2M-33	247	27.2	5.6	1.0	2.5	0.5	1.4	23.9	53.7	7.0	30.1	7.8	
K2M-35	268	29.9	5.9	0.6	2.7	0.5	1.4	25.1	55.9	7.3	31.1	8.0	
K2M-49	272	30.5	5.0	0.7	3.0	0.5	1.6	24.7	54.8	7.2	30.6	7.8	
K2M-50	251	26.4	5.4	0.8	2.4	0.5	1.4	21.5	48.1	6.4	27.3	7.1	
K2M-52	262	28.7	3.9	0.7	2.7	0.6	1.4	23.6	53.0	6.8	29.5	7.6	
K2M-56	277	31.0	5.9	1.2	2.8	0.6	1.5	25.7	57.5	7.3	30.1	7.7	
K2M-57	295	33.4	5.7	0.9	2.8	0.6	1.6	27.2	61.4	7.6	31.5	8.1	
K2M-59	274	30.4	5.4	0.9	2.6	0.6	1.4	24.1	55.2	7.0	28.8	7.5	
ICP precision													
std dev (ppm)			0.426672	0.378837	0.021175	0.004036	0.003385	0.50816	0.94443	0.168613	0.583129	0.242432	
%RSD			7.197001	52.99142	0.710854	0.605076	0.2135	1.787669	1.477834	2.116095	1.776163	2.896904	

Table 2 (cont.)

Sample	ICP	Zr/Hf								
	Eu	Gd	Tb	Dy	Ho	Er	Tm	Yb	Lu	
K2M-1	2.6	8.6	1.3	7.6	1.4	3.9	0.5	3.2	0.5	48.747833
K2M-3	3.0	9.7	1.5	8.8	1.6	4.5	0.5	3.7	0.5	46.660326
K2M-5	2.9	9.7	1.5	8.7	1.7	4.5	0.5	3.7	0.5	47.898452
K2M-10	2.1	6.6	1.0	6.0	1.1	3.0	0.3	2.5	0.4	45.318729
K2M-12	2.8	8.9	1.4	8.2	1.6	4.1	0.5	3.5	0.5	46.971407
K2M-15	2.5	7.8	1.3	7.2	1.4	3.7	0.4	3.1	0.4	45.049099
K2M-18	2.4	7.6	1.2	7.0	1.3	3.5	0.4	2.9	0.4	47.115955
K2M-20	2.4	7.8	1.2	7.0	1.3	3.5	0.4	2.9	0.4	46.245303
K2M-21	2.5	8.1	1.3	7.3	1.4	3.7	0.4	3.1	0.4	48.129471
K2M-22	2.5	8.0	1.3	7.3	1.4	3.8	0.4	3.1	0.5	48.757179
K2M-25	2.3	7.2	1.1	6.6	1.2	3.3	0.4	2.8	0.4	49.0027
K2M-26	2.6	8.4	1.3	7.7	1.4	3.9	0.4	3.2	0.5	43.00494
K2M-29	2.5	7.6	1.3	7.0	1.3	3.7	0.4	3.0	0.4	57.284946
K2M-33	2.6	8.2	1.3	7.5	1.4	3.9	0.4	3.2	0.5	43.785953
K2M-35	2.7	8.3	1.3	7.7	1.4	4.0	0.5	3.2	0.5	45.486867
K2M-49	2.5	8.0	1.3	7.4	1.4	3.8	0.4	3.1	0.5	54.342454
K2M-50	2.4	7.3	1.1	6.4	1.2	3.1	0.4	2.5	0.4	46.160725
K2M-52	2.5	7.9	1.3	7.2	1.4	3.7	0.4	3.1	0.5	66.662855
K2M-56	2.4	7.8	1.2	7.2	1.3	3.6	0.4	3.0	0.4	46.964748
K2M-57	2.6	8.2	1.3	7.5	1.4	3.8	0.4	3.1	0.5	52.109556
K2M-59	2.3	7.5	1.2	6.8	1.3	3.4	0.4	2.9	0.4	51.069193
ICP precision										
std dev (ppm)	0.040593	0.199251	0.04642	0.182584	0.041082	0.10926	0.016252	0.062169	0.011712	
%RSD	1.543456	2.318188	3.459786	2.398142	2.841361	2.803835	3.600227	1.925427	2.482965	

All Fe as Fe_2O_3 *

$$Mg \# = Mg / (Mg + Fe^{2+})$$

LOI = Loss on ignition (wt. %) is the sample weight lost after 30 minutes at 1020°C

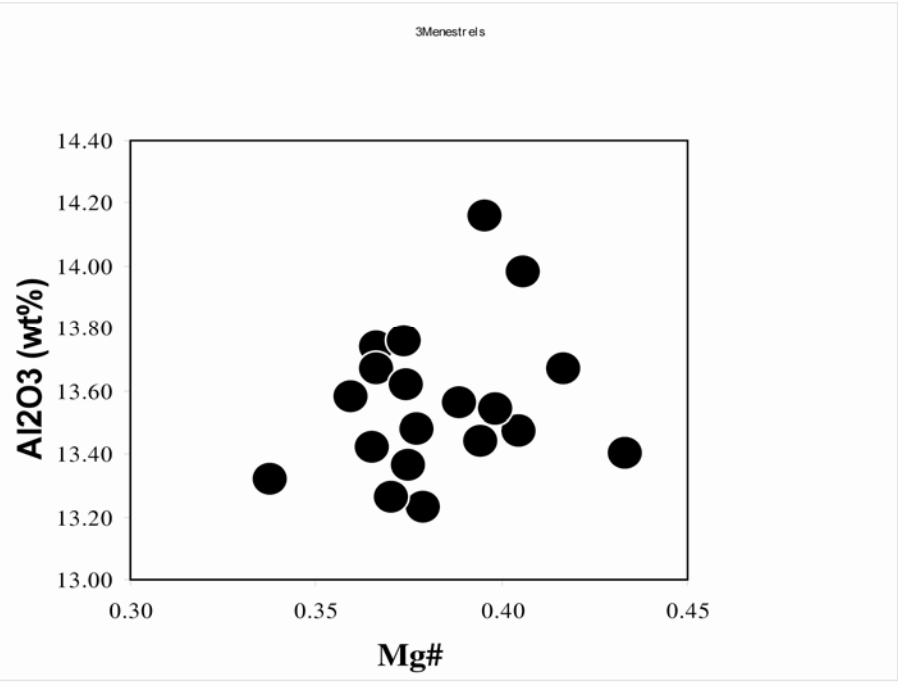
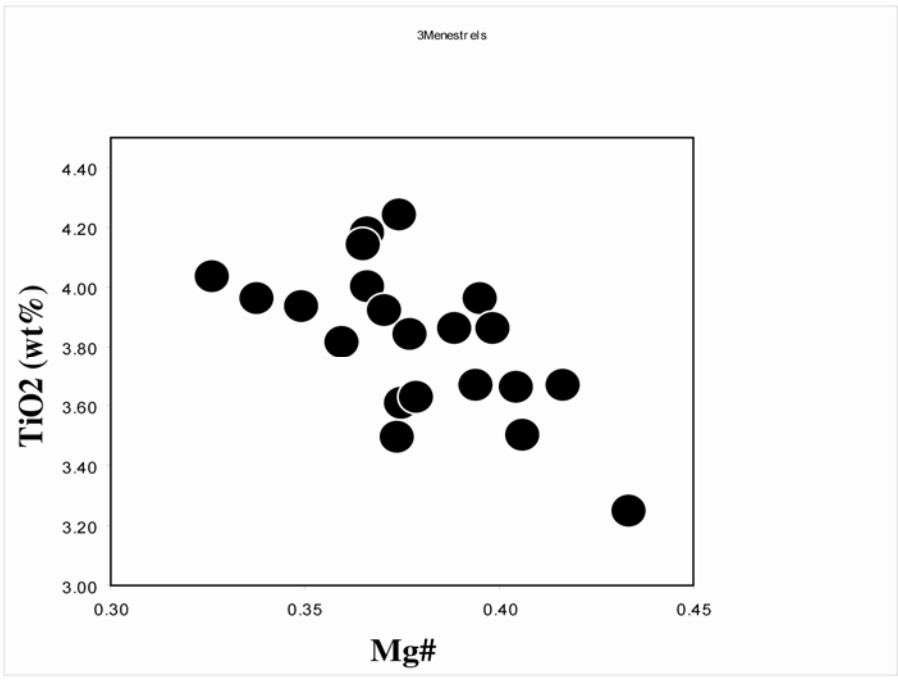
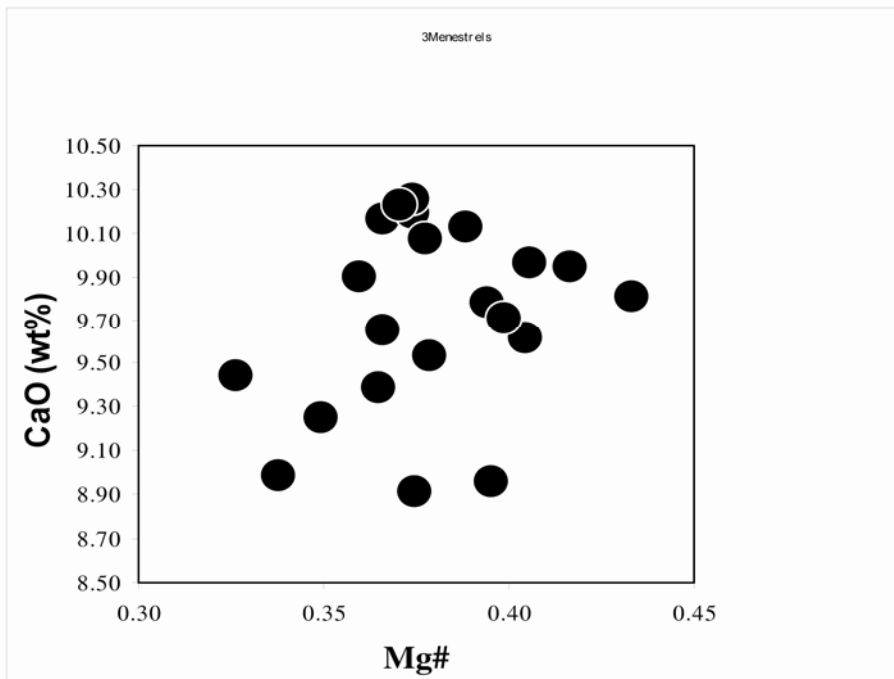
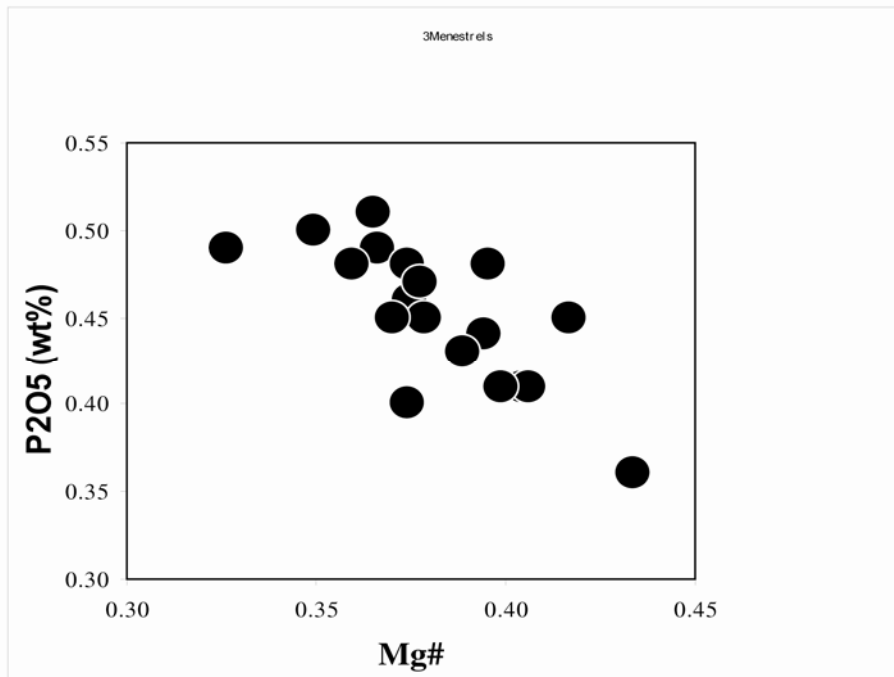
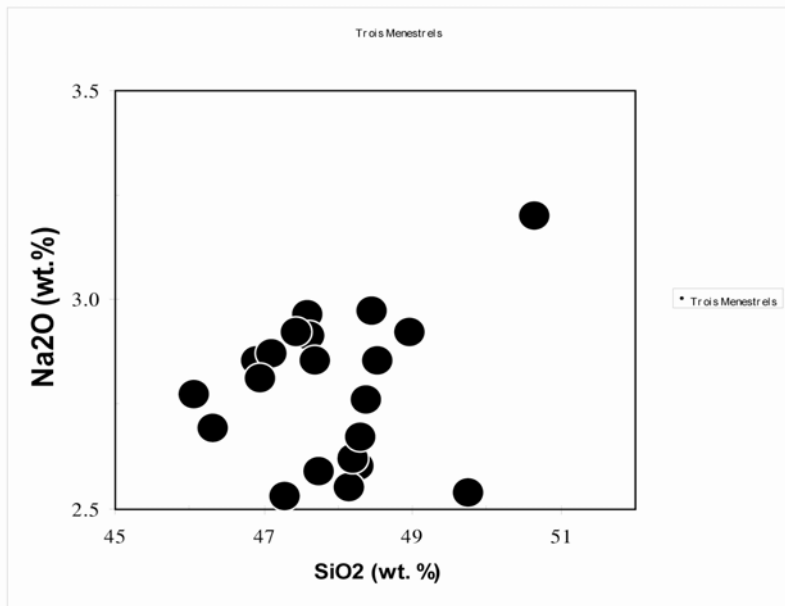
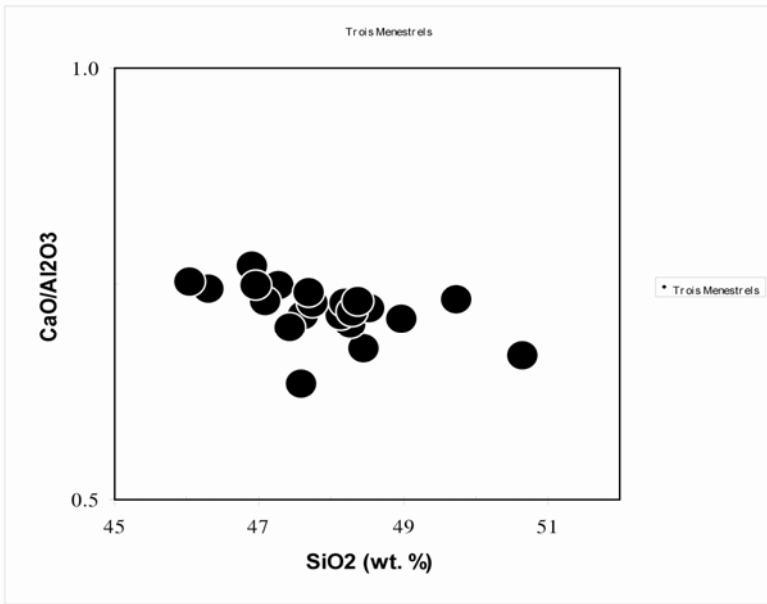


Figure 8. Major elements (all in wt. %) vs. Mg# and vs Silica. All samples define a negative trend for TiO₂-Mg# and P₂O₅-Mg# consistent with control of lava compositions by apatite and Fe-Ti oxide fractionation (see also Fig. 5). But there is considerable scatter with no distinction between Al₂O₃ and CaO plots vs. Mg#.





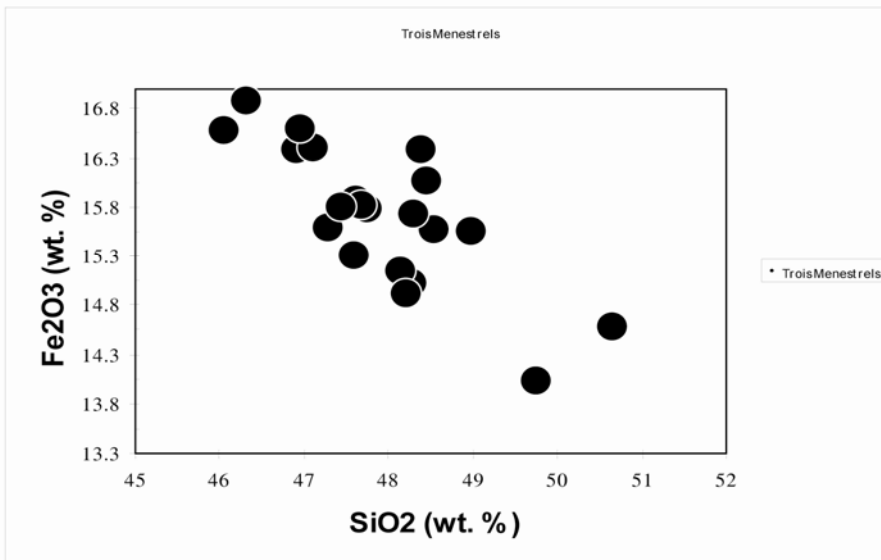
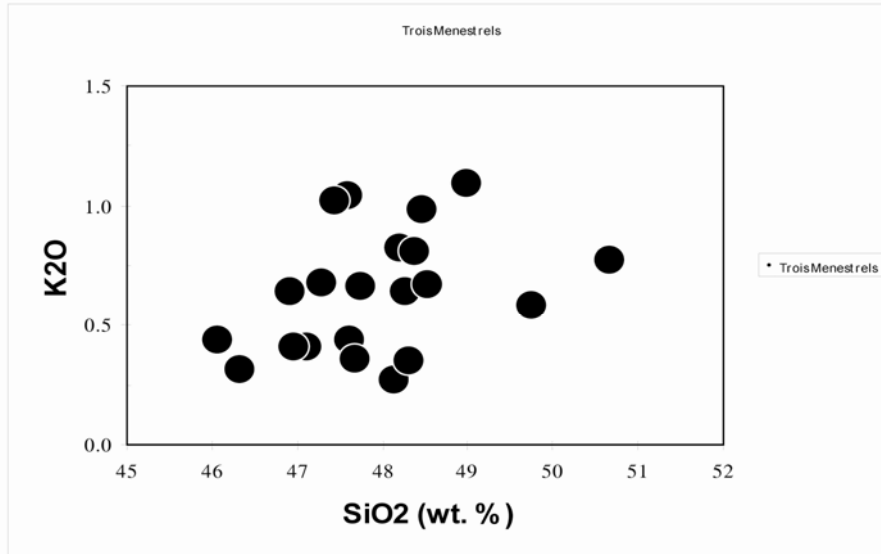


Figure 8 continued. Variation in SiO₂ vs. CaO/Al₂O₃, Na₂O, K₂O and Fe₂O₃ (all in wt. %) for samples from Mt. Les Trois Menestrels section. Note that CaO/Al₂O₃ shows a slight decrease with increasing SiO₂, and Fe₂O₃ constantly decreases with increasing SiO₂ as a consequence of olivine, clinopyroxene and titanomagnetite crystallization. K₂O and Na₂O slightly increase but some samples show Na₂O depletion, which may be interpreted as an alteration effect.

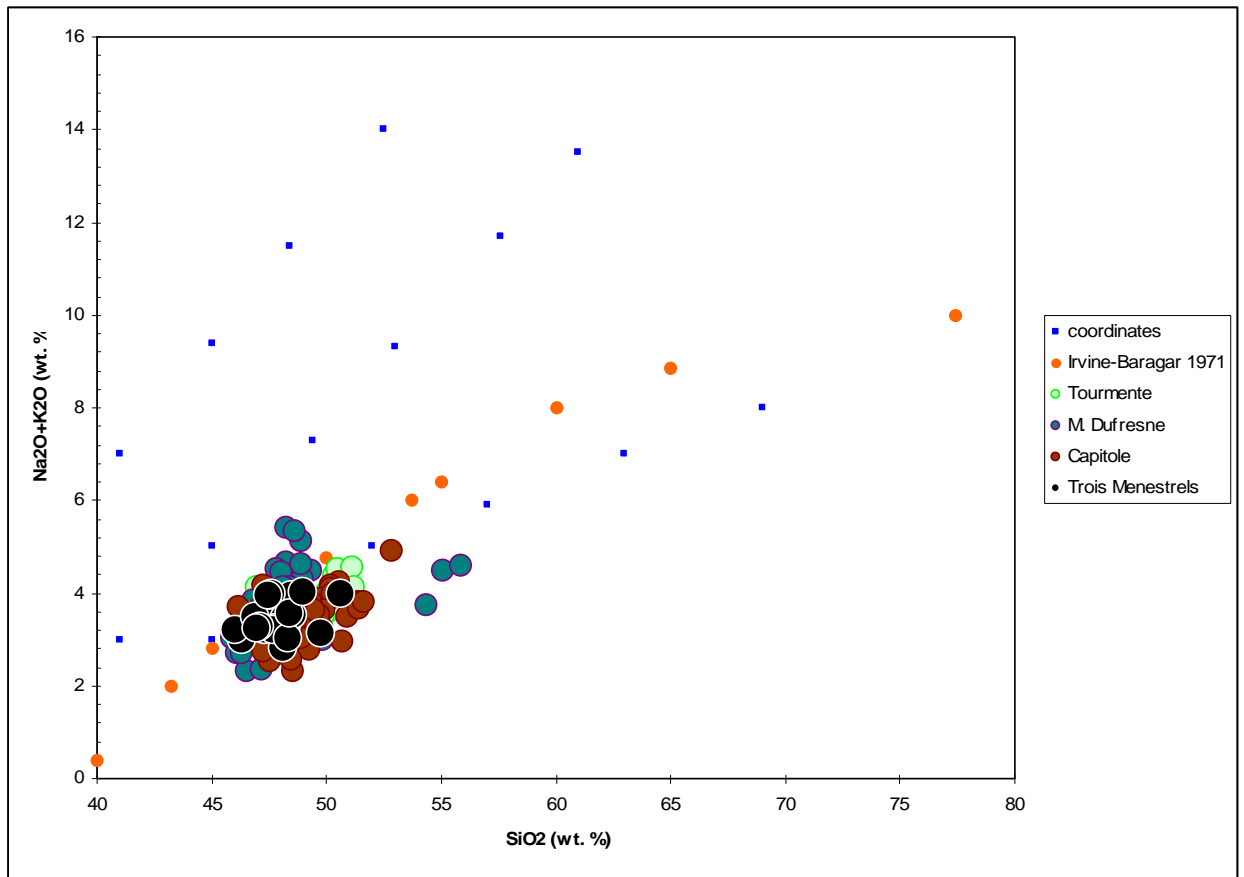


Figure 9. Total alkalis vs. SiO₂ classification diagram showing the Plateau Central of the Kerguelen Archipelago (classification boundaries from Le Maitre et al., 1989 and Irvine and Baragar, 1971). Sample compositions from Trois Menestrels are blue diamonds. The ~26-25 Ma Mt. Tourmente (Frey et al., 2002), Capitole (Xu et al., 2007), Marion Dufresne (Annell et al., 2006) and Crozier (Frey et al., 2002) basalts are plotted in comparison. The Mt. Tourmente, Capitole and most Marion Dufresne basalts closely overlap with measured compositions at Mt. Les Trois Menestrels and straddle the alkalic-tholeiitic boundary.

Trace element geochemistry

Positive linear correlation at Mt. Trois Menestrels is illustrated in Fig. 10 between Mg#, Ni and Cr that are consistent with both olivine and pyroxene fractionation to form low-MgO basalts; however olivine is not frequent in most of the thin sections (Table 1). Olivine must therefore be a residue of crystal fractionation at depth. Sr (compatible in plagioclase) abundances are nearly constant and are not positively correlated with abundances of an incompatible element, such as Nb.

Normalization to an ideal primitive mantle composition (Sun and McDonough, 1989) and correlation of trace element abundances estimates of shows important features (Fig. 11). This normalization removes the effect of the even-odd abundance characteristic inherited from solar fusion processes that created the elements of our solar system. A spider diagram shows all the trace element abundances simultaneously and here I illustrate just the most and least primary samples; i.e., these samples span the compositional range of the Mt. Les Trois Menestrels suite. Overall there is a slight negative slope from La to Lu (Fig. 11) suggesting that the mantle source, from which the TM magmas derived, consisted of typical peridotite without large amounts of garnet pyroxenite present. There is a slight relative depletion Sr that is symptomatic of slight amounts of plagioclase fractionation. Rb shows the largest difference between more primary and less primary basalt compositions creating wide variation in Ba/Rb (range = 13.3-450). These ratios result from extremely low Rb abundances, particularly for samples K2M-18, K2M-22, K2M-29 and K2M-50. This may stem from post-emplacement fluid removal of the Rb.

Elements that can potentially be mobile during alteration of basaltic rocks such as Ba, Nb, Zr, Y, Ce, U, and Pb, define positive linear correlations with Nb – an extremely immobile element; the positive linear correlation between immobile and mobile elements indicates that

trace element concentrations have not been significantly affected by secondary alteration (Fig. 13).

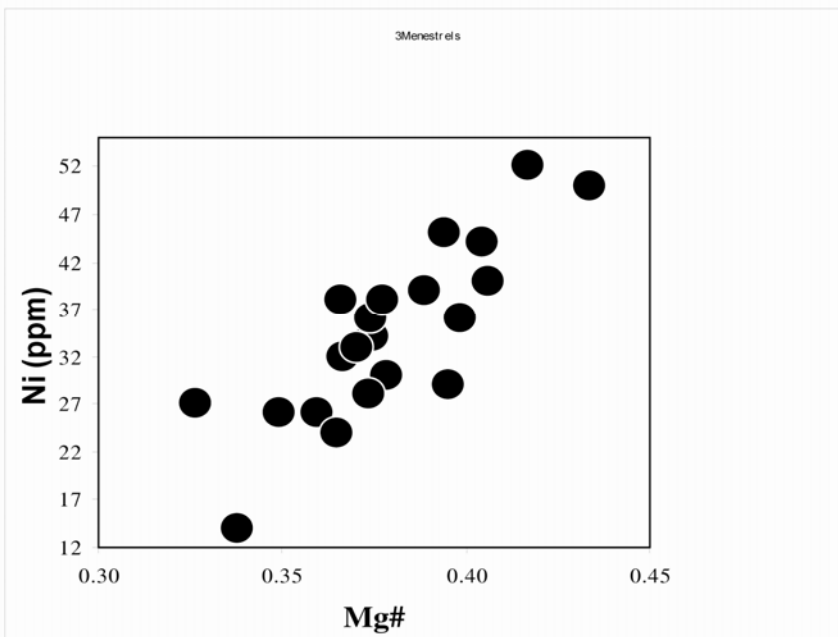
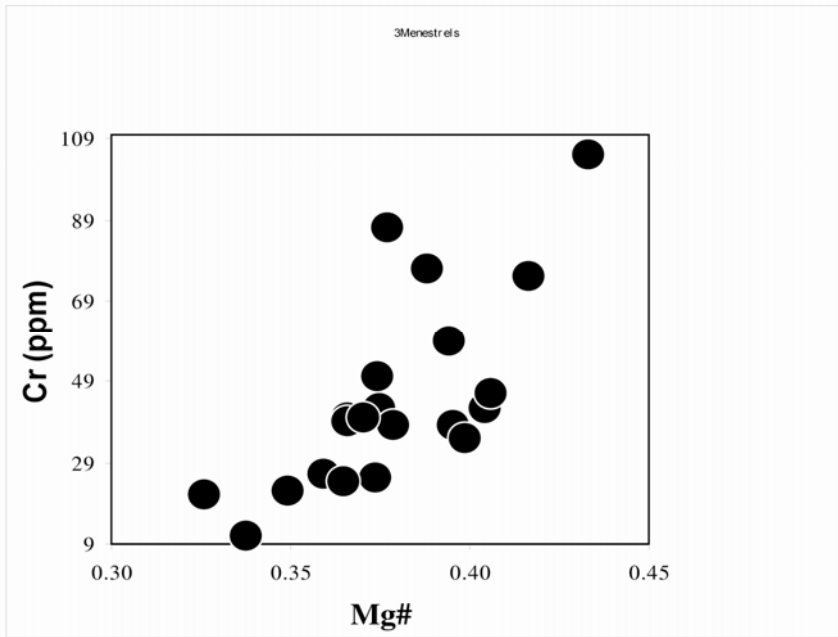


Figure 10 Cr and Ni abundance in (ppm) vs. Mg# in Mt. Les Trois Menestrels. The positive correlations between MgO and Ni and Cr are consistent with olivine +/-or clinopyroxene fractionation.

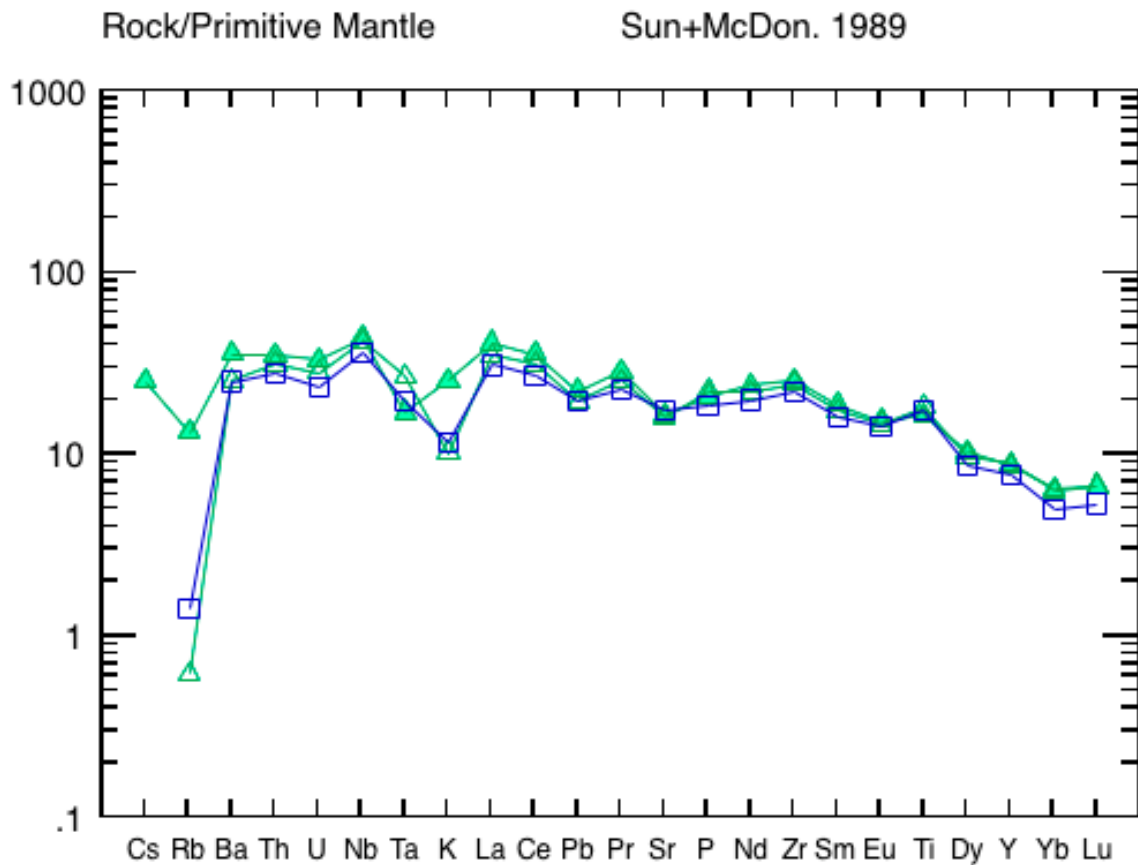


Figure 11. Incompatible element abundances in selected samples from Mt. Les Trois Menestrels Basalts normalized to primitive mantle estimates of Sun & McDonough (1989). Filled and open triangles represent the average estimate of K2M-1 and K2M-50, the most differentiated samples of this study. Squares represent the average estimate of a less differentiated sample (K2M-22). Important features are the negative slopes from Nb to Yb with a pronounced relative depletion in K and large variation in Ba/Rb generally caused by Rb depletion.

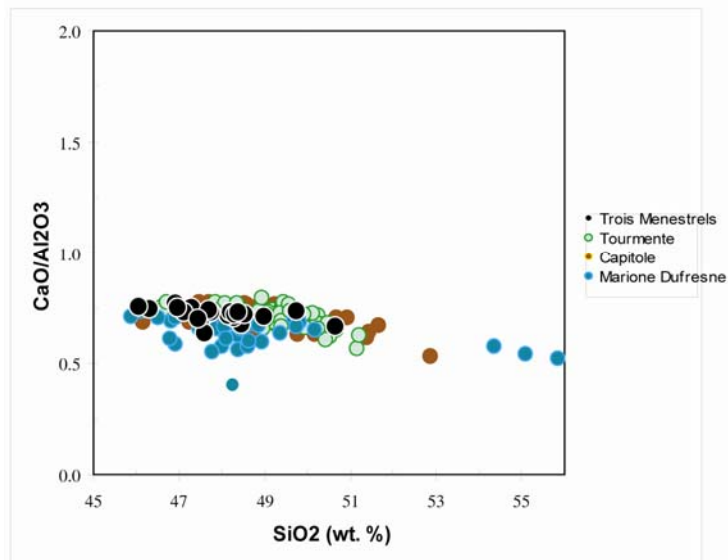
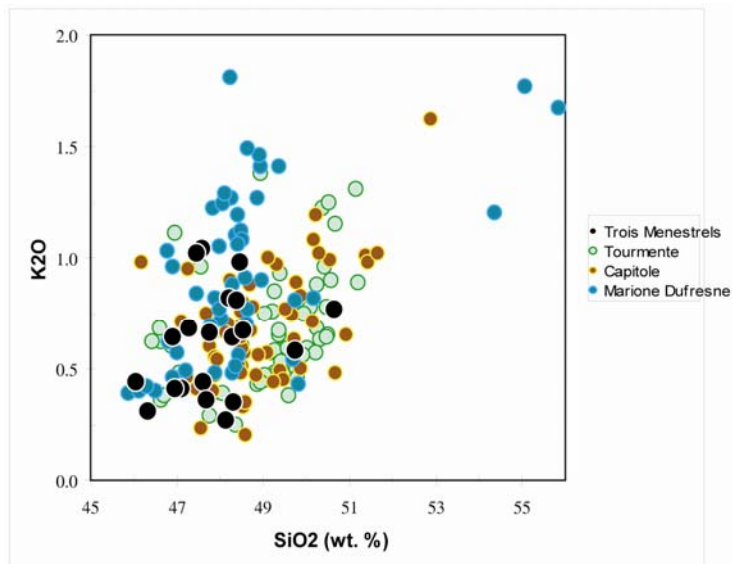
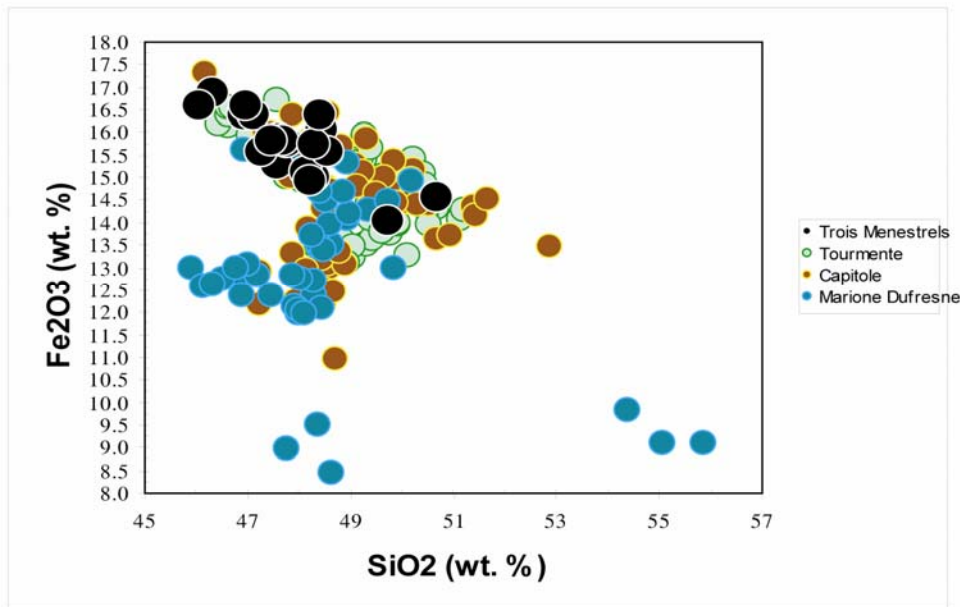
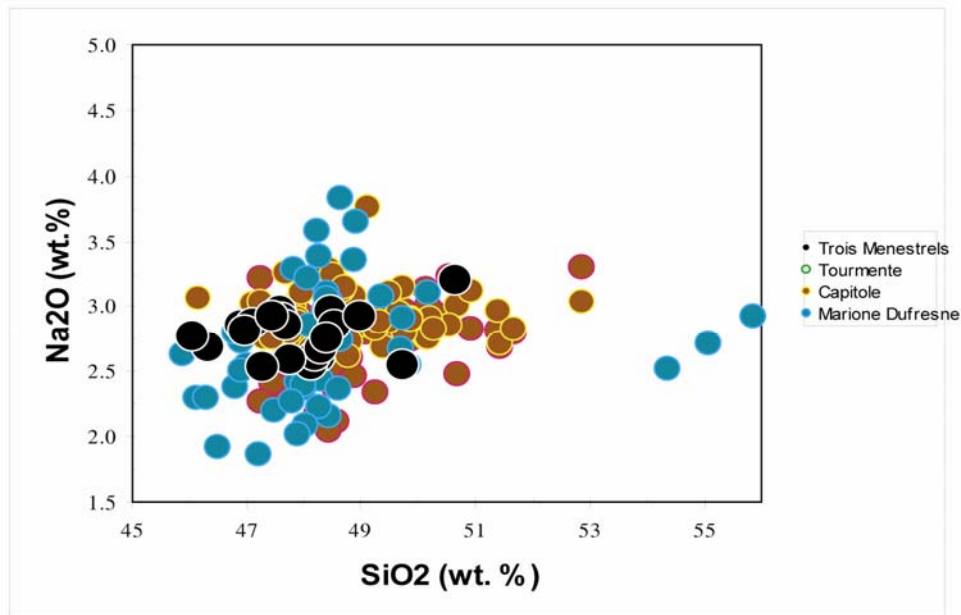
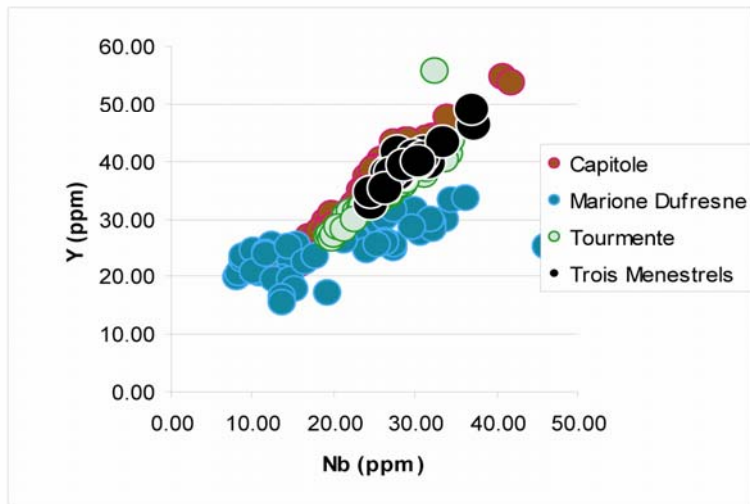
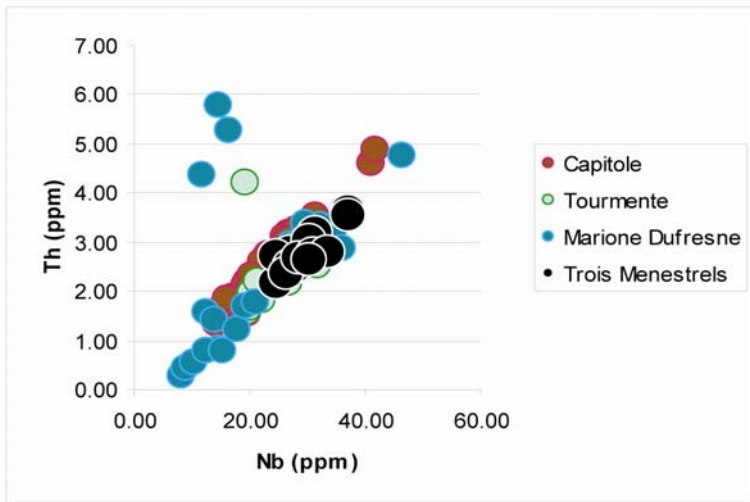


Figure 12. Fe_2O_3 , K_2O , $\text{Al}_2\text{O}_3/\text{CaO}$ and Na_2O vs. SiO_2 diagrams (all oxides in wt. %) for Mt. Les Trois Menestrels, Tourmente, Capitole and Marion Dufresne. A clear fractionation trend of Fe-Ti oxides is observed.

Figure 12 continued





**Figure 13. Abundances of Ce, Y, Zr, U, Ba and Th vs. Nb content (all in ppm).
The good correlation with Nb of these elements sensitive to post magmatic alteration suggests that Mt. Les Trois Menestrels and the Plateau Central in general have not been significantly disturbed by secondary alteration.**

Figure 13 continued

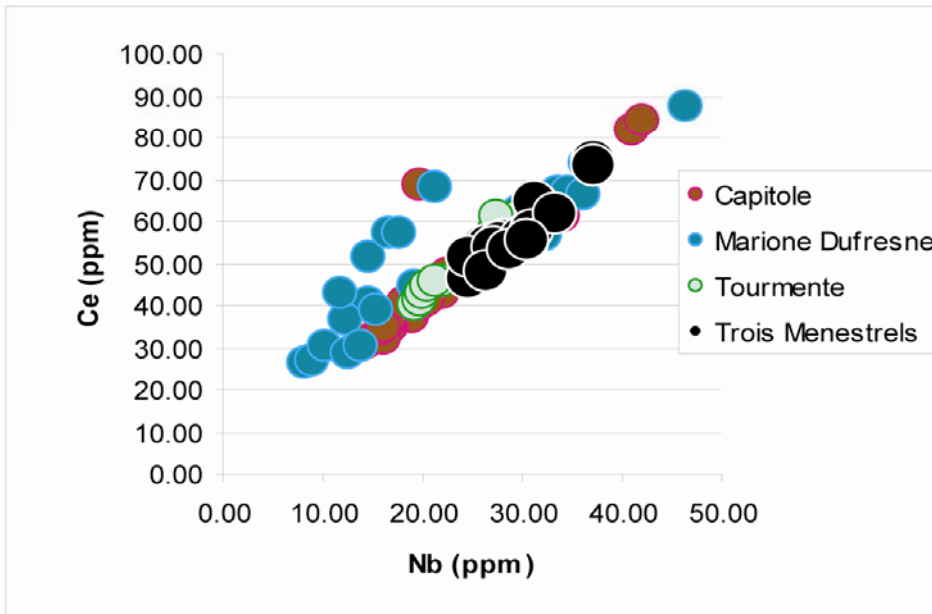
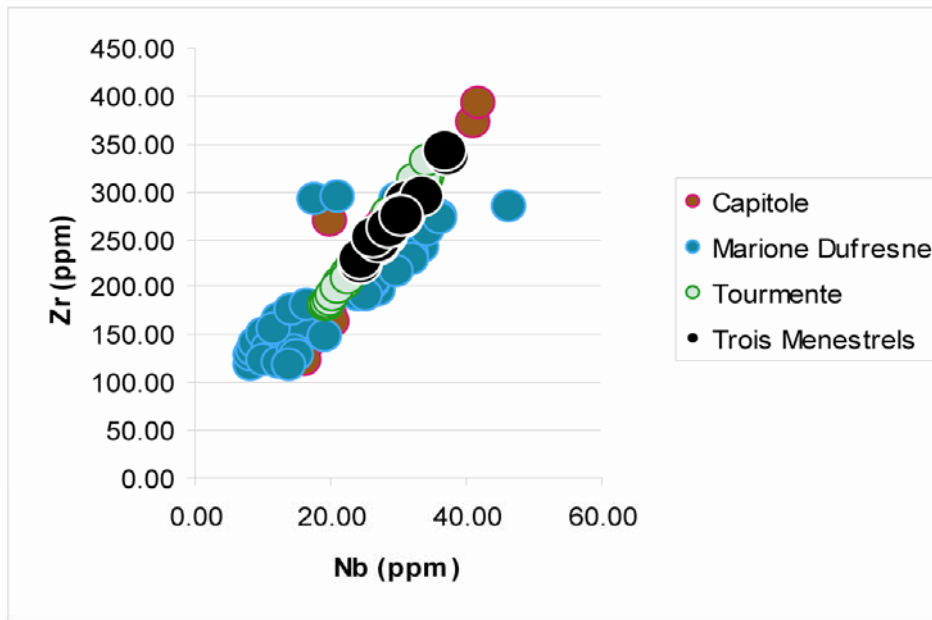
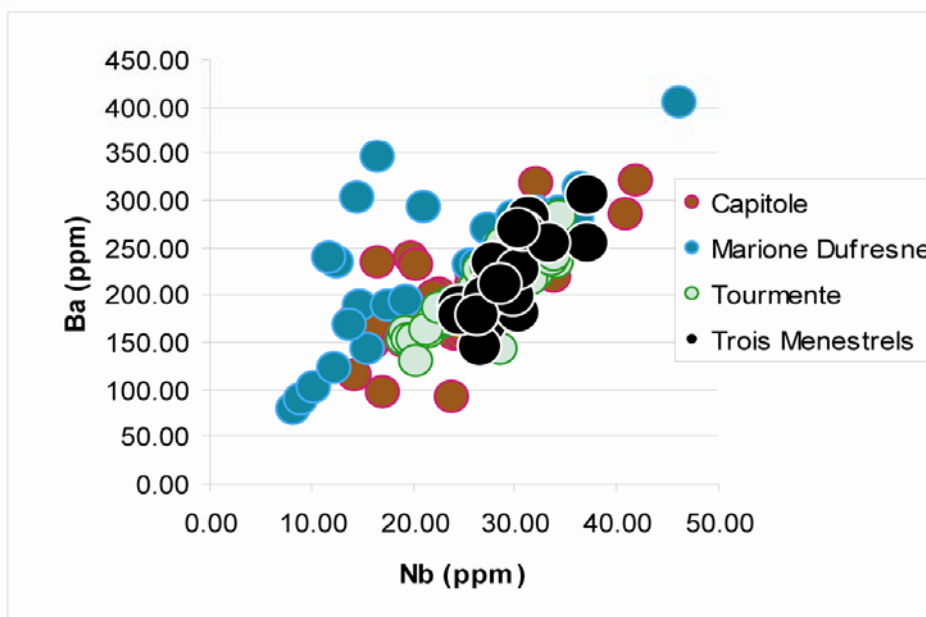
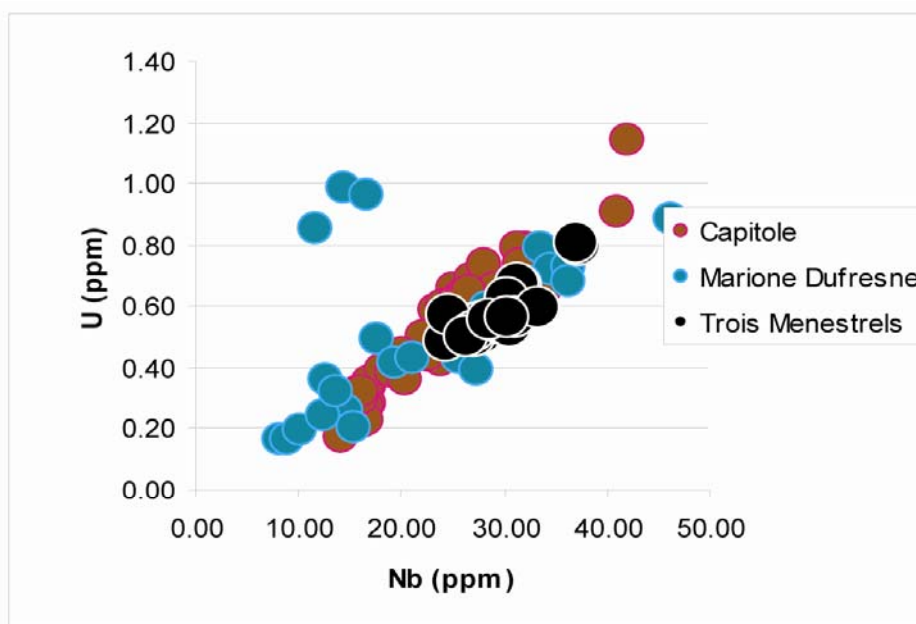


Figure 13 continued



Stratigraphic variations in trace element compositions are illustrated in Fig. 14. Two of the three units identified in Table 1 are immediately apparent.

Isotopic composition

Isotopic data are listed in Table 3 and plotted in Figs. 15-16-17. The initial $^{87}\text{Sr}/^{86}\text{Sr}$ and $^{143}\text{Nd}/^{144}\text{Nd}$ are negatively correlated; measured values are relatively uniform; except for one sample K2M-50 (finer-grained basalt), with higher Sr isotope ratios (0.705125) and lower Nd isotope ratios (0.512647), $^{87}\text{Sr}/^{86}\text{Sr}$ range only from 0.704654838 to 0.704838 and $^{143}\text{Nd}/^{144}\text{Nd}$ from 0.512672 to 0.512744. K2M-50 has the highest $^{87}\text{Sr}/^{86}\text{Sr}$ value observed in all four sections studied; except Mt. Marion Dufresne, the least $^{143}\text{Nd}/^{144}\text{Nd}$ (0.512672) as well as low radiogenic $^{206}\text{Pb}/^{204}\text{Pb}$. Mt. Trois Menestrels flood basalts display variations in both $^{87}\text{Sr}/^{86}\text{Sr}$ and $^{143}\text{Nd}/^{144}\text{Nd}$, defining a range similar to those observed at Mt. Capitole and Mt. Tourmente from the Plateau Central of the Kerguelen Archipelago and typically plot along the trend define by the extreme isotopic variation generated by the overall Kerguelen Archipelago flood basalts Fig. 15. The initial ϵ_{Nd} vs. ϵ_{Hf} values are positively correlated, spanning a small range from +0.67 to +2.08 and +3.23 to +5.74, respectively Fig. 17. The Pb isotopic compositions are also positively correlated, variations in Pb isotopic compositions for samples from Les Trois Menestrels basaltic section show, as expected, a close relationship with sections of the Plateau Central. The samples overlap those from Mt. Capitole and define the same trend with similar slope in plot of $^{208}\text{Pb}/^{204}\text{Pb}$ vs. $^{206}\text{Pb}/^{204}\text{Pb}$ (Fig. 16). Here also the sample K2M-50 is distinguished from the others, by recording the lowest radiogenic Pb isotope composition observed in this study ($^{206}\text{Pb}/^{204}\text{Pb} = 18.2425$).

Comparison with other parts of the Kerguelen Plateau Central

Except for Mt. Marion Dufresne, Mt. Trois Menestrels section has major and trace element abundances plus isotopic compositions that are analogous with sections of similar age. I compare the geochemical characteristics of the Mt. Trois Menestrels lavas to previously studied sections from the Plateau Central (Mt. Tourmente, Mt. Capitole and Mt. Marion Dufresne) in order to determine the level of heterogeneity of the source rocks at 25 Ma.

In general, compositions of Mt. Trois Menestrels lavas overlap fields for previously studied Kerguelen Archipelago of the same age; Mt. Capitole, Mt. Tourmente and Mt. Marione Dufresne. Six Marion Dufresne samples deviate from this trend: three samples (93-539 to 93-540) are characterized by relatively high SiO₂ contents and are below the alkalic-tholeiitic boundary; three others (93-533, 93-576 and 577) are more alkalic and plot above the line. Eight out of 45 samples from Mt. Crozier overlap with Mt. Trois Menestrels basaltic composition (Fig.9).

In general, the isotopic homogeneity of samples from Mt. Trois Menestrels, fall in the same range with those from Mt. Tourmente and Mt. Capitole. All the three sections contrast with the isotopic diversity from older sections located in the north of the Archipelago (Mt. Fontaine, Mt. des Ruches, and Mt. Rabouillere) and younger rocks (Mt. Crozier).

Table 3 Sr, Nd, Hf and Pb isotopic data of Mt. Les Trois Menestrels

	87Sr/86Sr	2 SE	143Nd/144Nd	2 SE	eps Nd	176Hf/177Hf	2 SE
K2M-1	0.704806	0.000009	0.512715	0.000005	1.51	0.282914	0.000004
K2M-3	0.704856	0.000010	0.512713	0.000005	1.47	0.282911	0.000007
K2M-5	0.704787	0.000008	0.512712	0.000005	1.45	0.282916	0.000004
K2M-10	0.704785	0.000007	0.512725	0.000005	1.71	0.282914	0.000006
K2M-12	0.704768	0.000007	0.512725	0.000009	1.71	0.282914	0.000004
K2M-15	0.704749	0.000007	0.512740	0.000006	2.00	0.282934	0.000005
K2M-18	0.704658	0.000007	0.512732	0.000010	1.84	0.282934	0.000010
<u>K2M-20</u>	<u>0.704686</u>	<u>0.000007</u>	0.512738	0.000006	1.96	0.282911	0.000005
K2M-21	0.704681	0.000007	0.512737	0.000007	1.94	0.282914	0.000010
						0.282926	0.000008
K2M-22	0.704687	0.000008	0.512730	0.000006	1.80	0.282934	0.000007
K2M-25	0.704743	0.000007	0.512730	0.000006	1.80	0.282919	0.000003
K2M-26	0.704681	0.000007				0.282933	0.000008
K2M-29	0.704703	0.000007	0.512744	0.000006	2.08	0.282923	0.000011
K2M-35	0.704696	0.000007	0.512734	0.000006	1.88	0.282926	0.000004
K2M-39	0.704692	0.000007	0.512723	0.000006	1.67	0.282920	0.000008
K2M-49	0.704714	0.000007	0.512729	0.000006	1.78	0.282923	0.000004
K2M-50	0.705125	0.000007	0.512672	0.000006	0.67	0.282863	0.000004
<u>K2M-52</u>	<u>0.704737</u>	<u>0.000008</u>	0.512723	0.000009	1.67	0.282916	0.000008
K2M-53	0.704853	0.000007					
K2M-56	0.704815	0.000007	0.512709	0.000006	1.39	0.282910	0.000009
K2M-57	0.704808	0.000007	0.512711	0.000006	1.43		
K2M-59	0.704834	0.000008	0.512702	0.000006	1.26	0.282904	0.000008
K2M-59#2	0.704853	0.000007				0.282899	0.000023
BE			0.512638			0.282772	
BHVO-2#1	0.703453	0.000008	0.512984	0.000006	6.76	0.283108	0.000004
BHVO-2#2	0.703466	0.000007	0.512981	0.000006	6.70		

	eps Hf	206Pb/204Pb	2 SE	207Pb/204Pb	2 SE	208Pb/204Pb	2 SE
K2M-1	5.01	18.4243	0.0012	15.5404	0.0010	38.8575	0.0028
K2M-3	4.92	18.3739	0.0009	15.5307	0.0009	38.7841	0.0022
K2M-5	5.08	18.3810	0.0006	15.5294	0.0006	38.7759	0.0019
K2M-10	5.04	18.4338	0.0006	15.5399	0.0006	38.8350	0.0015
K2M-12	5.01	18.3919	0.0006	15.5332	0.0005	38.8010	0.0016
K2M-15	5.74	18.4194	0.0008	15.5305	0.0007	38.8107	0.0019
K2M-18	5.72						
<u>K2M-20</u>	4.93	18.4163	0.0008	15.5378	0.0007	38.8086	0.0017
K2M-21	5.01	18.3743	0.0010	15.5315	0.0009	38.7609	0.0023
	5.46						
K2M-22	5.71	18.4113	0.0009	15.5378	0.0008	38.8345	0.0020
K2M-25	5.18	18.3918	0.0008	15.5372	0.0006	38.8190	0.0013
K2M-26	5.68	18.4659	0.0006	15.5425	0.0005	38.8567	0.0014
K2M-29	5.35	18.4564	0.0026	15.5459	0.0024	38.8488	0.0063
K2M-35	5.46	18.4579	0.0008	15.5453	0.0008	38.8763	0.0023
K2M-39	5.23	18.4509	0.0010	15.5436	0.0009	38.8926	0.0033
K2M-49	5.36	18.4211	0.0009	15.5414	0.0009	38.8772	0.0023
K2M-50	3.23	18.2425	0.0009	15.5347	0.0009	38.7759	0.0022
<u>K2M-52</u>	5.08	18.4020	0.0014	15.5421	0.0014	38.8673	0.0024
K2M-53							
K2M-56	4.87	18.4348	0.0007	15.5479	0.0006	38.8977	0.0015
K2M-57		18.4095	0.0005	15.5438	0.0005	38.8552	0.0016
K2M-59	4.66	18.4296	0.0009	15.5490	0.0008	38.8848	0.0022
K2M-59#2	4.49	18.4298	0.0007	15.5470	0.0006	38.8820	0.0015
BE							
BHVO-2#1	11.88	18.7036	0.0008	15.4988	0.0008	38.2061	0.0020
BHVO-2#2		18.6477	0.0008	15.4886	0.0009	38.2141	0.0017

Table 2. 2 continued: Sr, Nd, Hf and Pb isotopic data of Mt. Les Trois Menestrels

	Rb	Sr	Sm	Nd	Lu	Hf	Pb
K2M-1-1	8.48	351.00	8.40	32.80	0.47	5.90	1.59
K2M-3	6.30	354.00	9.64	38.20	0.54	7.20	1.83
K2M-5	7.70	388.00	9.40	37.10	0.54	7.20	1.86
K2M-10	11.70	368.00	6.42	24.80	0.36	4.92	1.17
K2M-12	8.39	364.00	8.80	34.10	0.49	6.15	1.35
K2M-15	4.43	350.00	7.60	28.50	0.44	5.50	0.80
K2M-18	1.46	387.00	7.50	28.50	0.42	5.24	1.27
K2M-20	9.00	360.00	7.50	28.80	0.42	5.49	1.33
K2M-21	5.50	359.00	7.90	30.40	0.44	5.28	1.29
K2M-22	0.90	357.00	7.80	29.90	0.46	5.60	1.43
K2M-25	5.50	358.00	7.13	27.40	0.39	5.20	1.23
K2M-26	5.80	363.00	8.00	30.40	0.46	5.70	1.33
K2M-29	2.22	380.00	7.47	28.50	0.43	4.02	1.32
K2M-35	4.81	347.00	7.80	30.10	0.46	5.64	1.37
K2M-39	5.89	356.00	8.00	31.10	0.48	5.89	1.39
K2M-49	1.70	361.00	7.80	30.56	0.46	5.01	1.57
K2M-50	1.28	364.00	7.10	27.33	0.35	5.44	1.43
K2M-52	6.00	337.00	7.60	29.50	0.46	3.90	1.45
K2M-56	7.26	352.00	7.70	30.10	0.44	5.90	1.52
K2M-57	8.20	325.00	8.10	31.50	0.45	5.66	1.58
K2M-59	18.60	333.00	7.50	28.80	0.41	5.37	1.37
	<i>18.60</i>	<i>333.00</i>	<i>7.50</i>	<i>28.80</i>	<i>0.41</i>	<i>5.37</i>	<i>1.37</i>

Table 3 continued: Sr, Nd, Hf and Pb isotopic data of Mt. Les Trois Menestrels

U	Th	$^{87}\text{Rb}/^{86}\text{Sr}$	$^{87}\text{Sr}/^{86}\text{Sr}$ 25 Ma	$^{147}\text{Sm}/^{144}\text{Nd}$	$^{143}\text{Nd}/^{144}\text{Nd}$ eps 25 Ma	Nd init	$^{176}\text{Lu}/^{177}\text{Hf}$
0.67	2.98	0.0699	0.704781	0.1548	0.512690	1.64	0.0113
0.80	3.61	0.0515	0.704838	0.1526	0.512688	1.61	0.0107
0.80	3.52	0.0574	0.704767	0.1532	0.512687	1.59	0.0107
0.49	2.17	0.0920	0.704753	0.1566	0.512700	1.83	0.0105
0.67	3.20	0.0667	0.704745	0.1560	0.512700	1.84	0.0113
0.51	2.57	0.0366	0.704736	0.1612	0.512714	2.11	0.0114
0.54	2.41	0.0110	0.704654	0.1591	0.512706	1.96	0.0114
0.54	2.49	0.0723	0.704661	0.1574	0.512713	2.08	0.0109
0.55	2.47	0.0443	0.704666	0.1571	0.512712	2.07	0.0118
0.63	2.66	0.0073	0.704685	0.1577	0.512705	1.93	0.0117
0.50	2.55	0.0445	0.704727	0.1573	0.512705	1.93	0.0106
0.50	2.79	0.0462	0.704665				0.0114
0.57	2.70	0.0169	0.704697	0.1585	0.512719	2.20	0.0152
0.52	2.51	0.0401	0.704682	0.1567	0.512709	2.01	0.0116
0.54	2.75	0.0479	0.704675	0.1555	0.512698	1.80	0.0116
0.53	3.03	0.0136	0.704709	0.1543	0.512704	1.92	0.0130
0.50	2.35	0.0102	0.705122	0.1571	0.512647	0.80	0.0091
0.56	2.68	0.0515	0.704719	0.1558	0.512698	1.80	0.0166
0.56	2.77	0.0596	0.704794	0.1547	0.512684	1.53	0.0106
0.60	2.81	0.0730	0.704782	0.1555	0.512686	1.56	0.0107
0.57	2.62	0.1616	0.704777	0.1574	0.512677	1.38	0.0108
0.57	2.62	0.1616	0.704796				

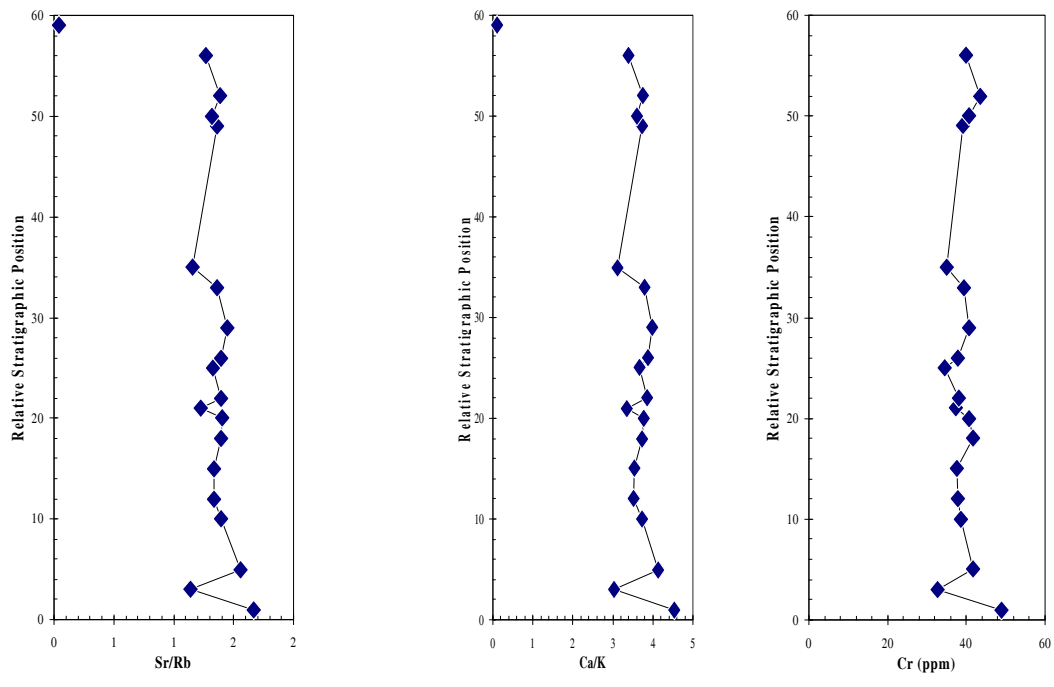


Figure 14. Stratigraphic distribution of Cr, Ca/K and Sr/Rb in the Mt. Les Trois Menestrels sections.

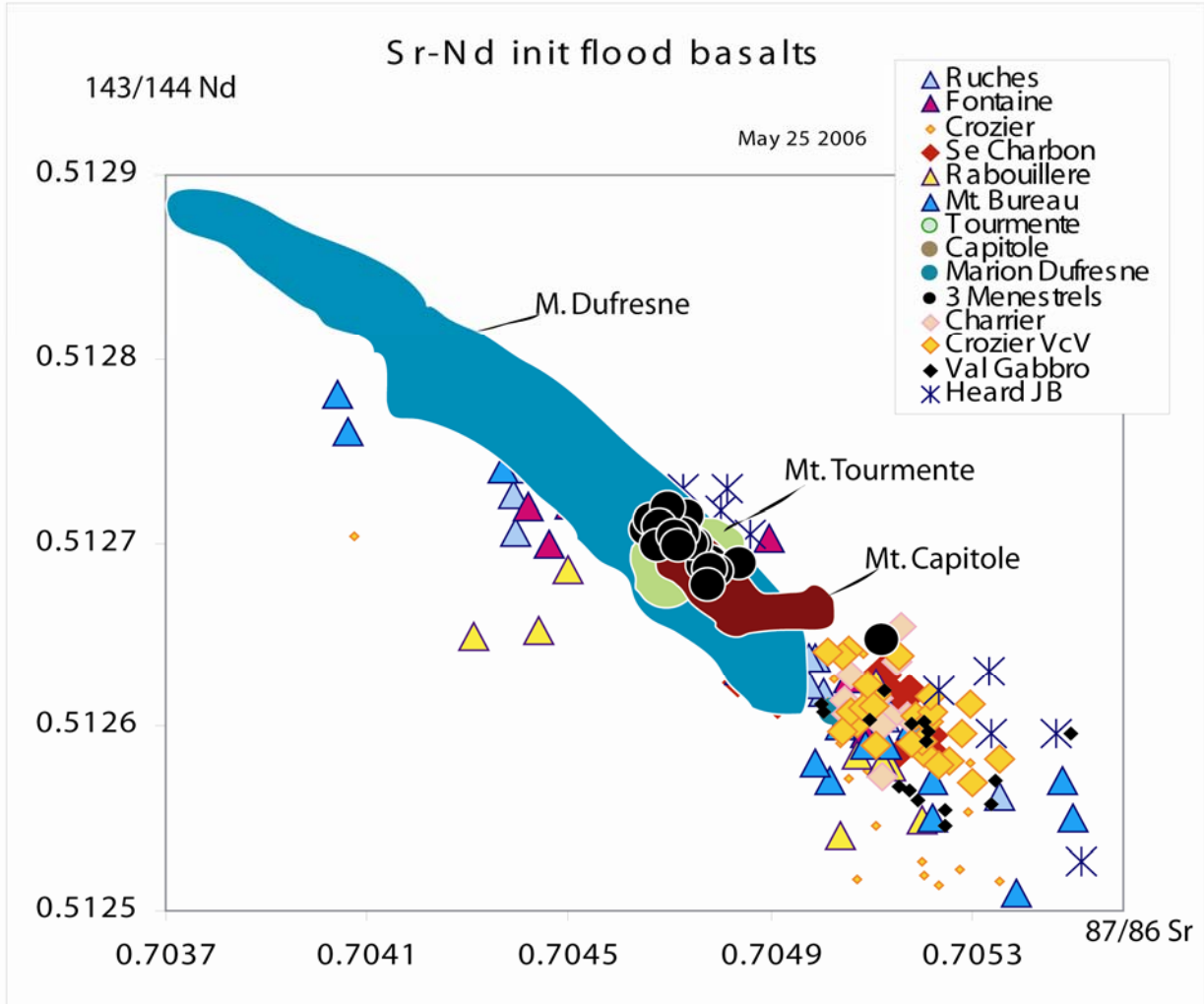


Figure 15. ($^{87}\text{Sr}/^{86}\text{Sr}$) vs. ($^{143}\text{Nd}/^{144}\text{Nd}$) from the Kerguelen Archipelago.

Mt. Trois Menestrels are shown in black circles, other fields are the studied sections from the entire Kerguelen Archipelago.

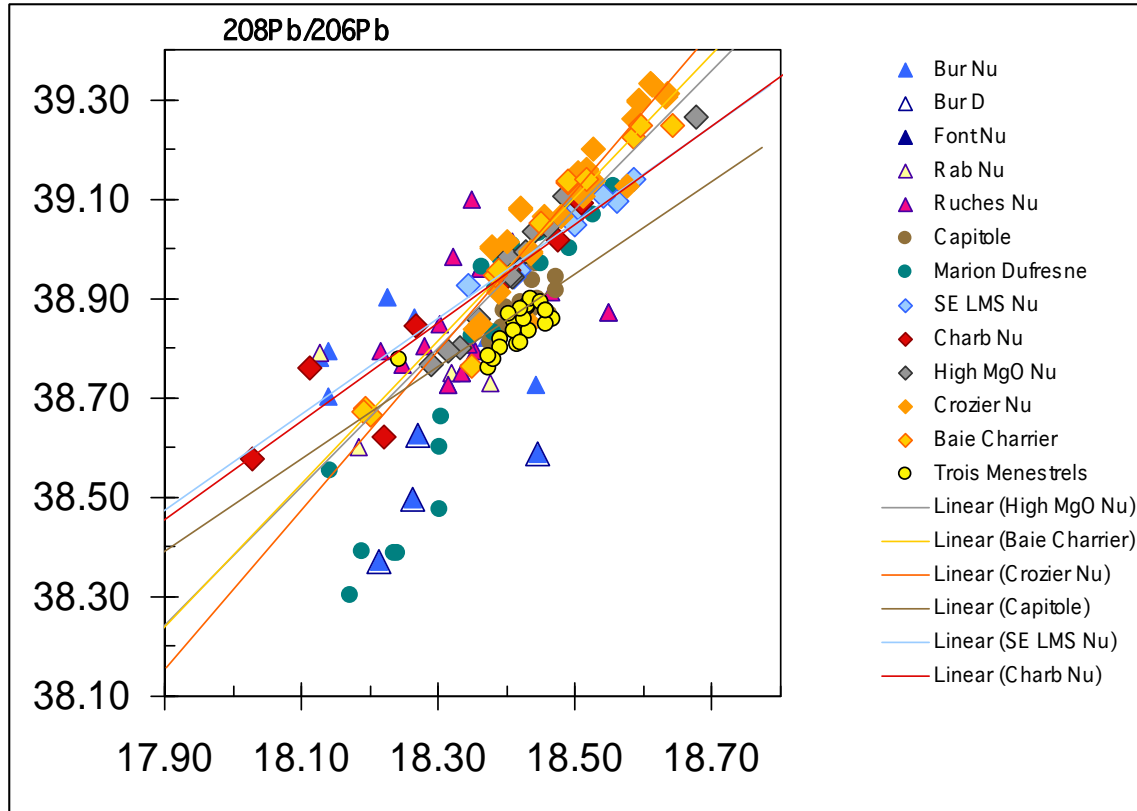


Figure 16. $^{208}\text{Pb}/^{204}\text{Pb}$ vs. $^{206}\text{Pb}/^{204}\text{Pb}$ data from Mt. LesTrois Menestrels and fields for various sections of the Kerguelen Archipelago.

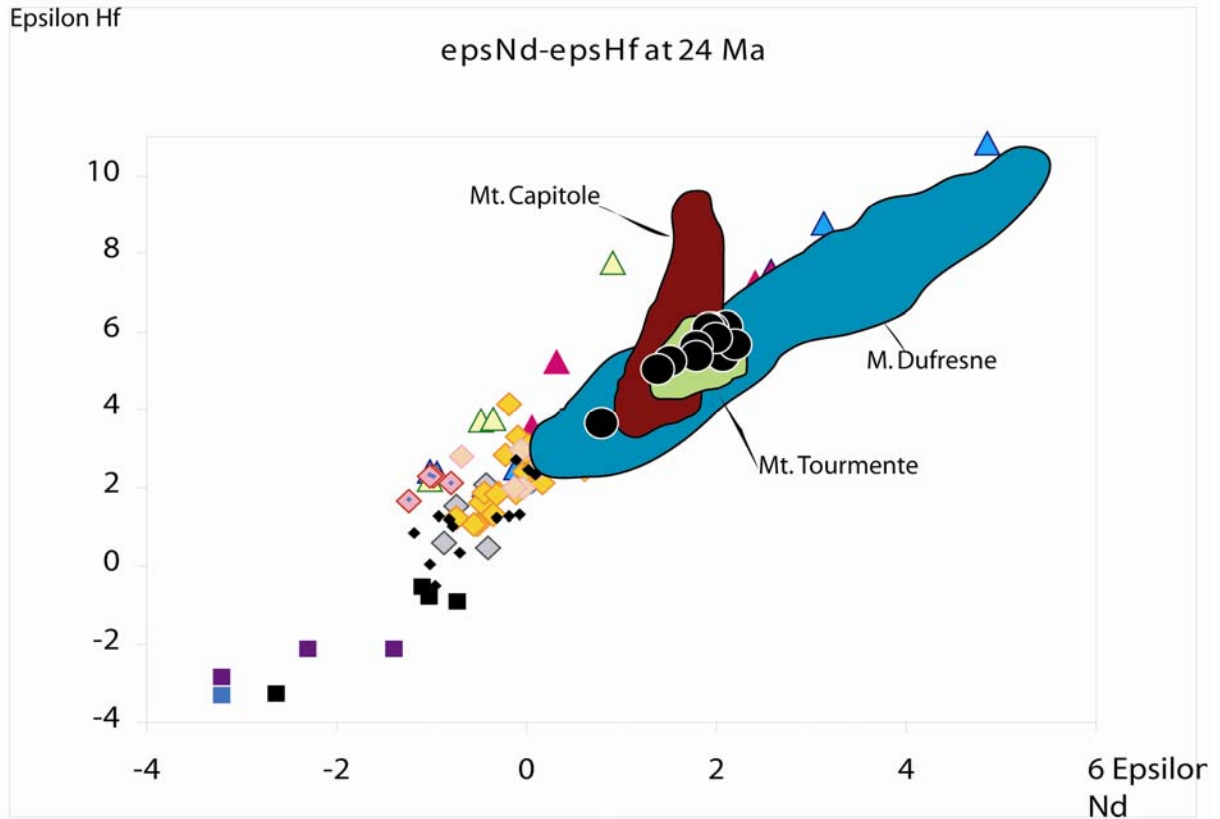


Figure 17. Epsilon_{Nd} vs. Epsilon_{Hf} in the Kerguelen Archipelago.

Lavas from Mt. Trois Menestrels are positively correlated, but do not extend into negative values for either ϵ_{Hf} or ϵ_{Nd} . Values are normalized to CHUR ($^{176}\text{Hf}/^{177}\text{Hf}_m = 0.282772$ and $^{143}\text{Nd}/^{144}\text{Nd}_m = 0.512638$; Wasserburg et al., 1981).

CHAPTER 5 - DISCUSSION

Mt. Trois Menestrels basaltic rocks have no to little geochemical evidence of alteration; most chemical characteristics are therefore likely to be primary igneous ones. However, despite the primary character of the lavas, Na contents may have been modified. Most samples have moderate to stronger depletion in Na₂O and, in general, a low to moderate abundance of K₂O (~0.7 wt. %) which may be interpreted as an alteration effect and therefore contrast the apparent tholeiitic composition of Trois Menestrels basalts. But this is not reflected by the low loss on ignition (0.3-2). In addition to Na₂O loss, CaO and MgO are higher in those samples (K2M-10-18-20-21-26-56; see table 2) and, loss of Na₂O seems to not result in apparent increase in SiO₂ (Fig. 9).

Like the flood basalts erupted in the different studied sections of the Plateau Central, the subalkalic tholeiitic basalts erupted at Mt. Les Trois Menestrels section are distinguished by their relatively low SiO₂ contents (Fig. 5), a result consistent with melt segregation from peridotite at relatively high pressure (e.g., Gaetani & Grove, 1998).

Most hafnium isotopic results demonstrate the important difference and similarity between the 25 Ma basaltic rocks from the Plateau Central in the Kerguelen Archipelago. The same linear array in the ϵ_{Hf} vs. ϵ_{Nd} plot corresponds to the same period of magmatic activity in flood basalts production Fig. 17. The higher ϵ_{Hf} basalts (Mt. Les Trois Menestrels, 80% of Mt. Tourmente, most of Mt. Marion Dufresne samples and Mt. Capitole) are tholeiitic and transitional, whereas the lower ϵ_{Hf} basalts (Mt. Crozier and part of Mt. Marion Dufresne) are dominantly alkalic. These sections are probably comagmatic; flood basalts volcanism on

Kerguelen Archipelago spanned at least 6 Ma and sections from the Plateau Central of the mid-to southeast of the archipelago are of the same approximate age. Although they do not have similar major phenocryst assemblage, they followed similar major element variation trends Fig. 12, have similar trace element characteristics (except for some of the Marion Dufresne measurements of MgO, SiO₂, Fe₂O₃, Sr, Th and U) as a result of similarity between parental magmas.

Isotopic heterogeneity for ocean-island basalt has generated big debate in the scientific community (for Hawaii: Lassister & Hauri, 1998; Keller et al., 2000; Regelous et al., 2002; for Iceland: Hanan et al., 2000; Kempton et al., 2000; for Galapagos: White et al., 1993; Blichert-Toft & White, 2001). Does this heterogeneity reflect difference within the plume or variation of component derived from the plume? In Kerguelen the contrasting results between the isotopic homogeneity of the ~25 Ma Plateau Central samples and the isotopic diversity from the rest of the Kerguelen Archipelago is consistent with this heterogeneity reflecting differences within the Kerguelen plume. The younger alkalic flood basalts from Mt. Crozier and part of Mt. Marion Dufresne representing the low melting component in the plume; the older transitional tholeiitic with a depleted component representing higher extents of melting.

CHAPTER 6 - CONCLUSION

Study of the mineral abundances, textures and geochemistry for subalkalic tholeiitic magmas that formed the 25Ma Mt. Les Trois Menestrels, of nearly 650m heights, on the Kerguelen Archipelago show several important trends. The section consists of fractionated basalts that are close to aphyric to very sparsely phyric, with minimal plagioclase variation (mainly groundmass); the variations are mostly due to change in apatite, titanomagnetite, plus some olivine and clinopyroxene crystallization. Basaltic lavas from Mt. Trois Menestrels are low-MgO basalts that did not show significant fractionation in magma reservoirs during ascent, single mineral aggregates (glomerocrysts) of plagioclase or plagioclase-olivine-clinopyroxene show that they were the only minerals precipitating from the magma at that stage of crystallization. Also normal zoning patterns of plagioclase in chain observed in some of the samples at Mt. Trois Menestrels indicate that the crystals had a brief period of independent crystallization before linking together.

Major, trace elements geochemistry and isotopic homogeneity from Mt. Trois Menestrels compared with the relative homogeneity of other sections from the Plateau Central of the Kerguelen Archipelago placed strong constraints on the history of the Kerguelen plume at 25 Ma. While debate continues over what these heterogeneities represent, alternative evidence supports heterogeneity intrinsic to the Kerguelen plume.

CHAPTER 7 - REFERENCES CITED

Annell, H., Scoates, J.S., and Weis, D., 2007, Petrology of the flood basalts at the tholeiitic-alkalic transition and phenocryst composition, Mt. Marion Dufresne, Kerguelen Archipelago, southern Indian Ocean. *Canadian Mineralogist* 45, 607-634.

Blichert-Toft, J. & White, W. M. 2001, Hf isotopic geochemistry of the Galapagos Islands. *Geochemistry, Geophysics, Geosystems* 2000GC000138.

Carbotte, S.M., Arko, R., Chayes, D.N., Haxby, W., Lehnert, K., O'Hara, S., Ryan, W.B.F., Weissel, R.A., Shipley, T., Gahagan, L., Johnson, K., Shank T. (2004), New Integrated Data Management System for Ridge2000 and MARGINS Research, *Eos Trans. AGU*, 85(51), 553, DOI: 10.1029/2004EO510002.

Charvis, P., & Operto, S., 1999, Structure of the Cretaceous Kerguelen volcanic province (southern Indian Ocean) from wide angle seismic data. *Journal of Geodynamics* 28, 51-71.

Damasceno, D., Scoates, J.S., Weis, D., Frey, F.A., Giret, A., 2002, Mineral chemistry of mildly alkalic basalts from 25 Ma Mont Crozier section, Kerguelen Archipelago: constraints on phenocryst crystallization environments. *Journal of Petrology* 43, 1389-1413.

Davies, H., Sun, S.S., Frey, F.A., Gautier, I., McCulloch, M., Price, R., Bassias, Y., Klootwijk, C.T., Leclaire, L., 1989, Basalt basement from Kerguelen Plateau and the trail of a DUPAL plume. *Contributions and Mineralogy and Petrology*. 103, 457- 469.

Doucet, S., et al., (2002), The depleted Mantle Component in the Kerguelen Archipelago basalts: Petrogenesis of Tholeiitic-Transitional Basalts from the Loranchet Peninsula, *Journal of Petrology* 43, 1341-1366.

Duncan, R.A., 1978, Geochronology of basalts from the Ninetyeast Ridge and Continental dispersion in the eastern Indian Ocean. *Journal of Volcanology and Geochemical Research* 4, 283-305.

Duncan, R.A., 2002, A timeframe for the construction of the Kerguelen Plateau and Broken Ridge. *Journal of Petrology*, 43, 1109-1119.

Frey, F.A. and Weis, D., 1995, Temporal evolution of the Kerguelen Plume: geochemical evidence from ~38 to 82 Ma lavas forming the Ninetyeast Ridge, *Contribution to Mineralogy and Petrology* 121, 12-28.

Frey, F.A., Coffin, M.F., Wallace, P.J. and the Leg 183 Shipboard Scientific Party, 2000a, Origin and Evolution of a Submarine Large Igneous Province: the Kerguelen Plateau and Broken Ridge, southern Indian Ocean, *Earth and Planetary Science Letters*, 176, 73-89.

Frey, F.A., Weis, D., Yang, H.-J., Nicolaysen, K., Leyrit, H. & Giret, A. 2000b, Temporal geochemical trends in the Kerguelen Archipelago basalts: evidence for decreasing magma supply from the Kerguelen plume. *Chemical Geology* 164, 61-80.

Frey, F.A., Nicolaysen, K., Kubit, B.K., Weis, D., & Giret, A., 2002, Flood basalt from Mt. Tourmente in the Central Kerguelen Archipelago: the change from transitional to alkalic basalt at ~25 Ma. *Journal of Petrology* 43, 1367-1387.

Gaetani, G.A., & Grove, T.L., 1998, The influence of water on melting of mantle peridotite. *Contributions to Mineralogy and Petrology* 131, 323-346.

Gautier, I., Weis, D., Mennessier, J.-P., Vidal, P., Giret, A., Loubet, M., 1990, Petrology and geochemistry of the Kerguelen Archipelago basalts (South Indian Ocean): evolution of the mantle sources from ridge to intraplate position. *Earth and Planetary Science Letters* 100, 59-76.

Geomapapp application available at www.geomapapp.org and www.marine-geo.org

Giret, A., 1983, Le plutonisme océanique intraplaque, exemple de l'archipel Kerguelen. Thèse doctorat d'état, Université Pierre et Marie Curie, Paris, 290 pp.

Giret, A., & Lameyre, J., 1983, A study of Kerguelen plutonism: petrology, geochronology and geological implications. In: Oliver, R.L., James, P.R. & Jago, J.B. (eds.) *Antarctic Earth Science*. Australia: Australian Academy of Sciences, pp.646-651.

Hanan, B.B., Blichert-Toft, J., Kingsley, R. & Schilling, J.-G., 2000, Depleted Iceland Mantle Plume Geochemical signature: artifact of multicomponent mixing? *Geochemistry, Geophysics, Geosystems* 1999GC000009.

Irvine, T.N., and Baragar, W.R.A., 1971, A guide to the chemical classification of the common volcanic rock. *Canadian Journal of Earth Sciences*, 8: 523-548.

Keller, R.A., Fisk, M.R. & White, W.M., 2000, Isotopic evidence for Late Cretaceous plume-ridge interaction at Hawaiian hotspot. *Nature* 405, 673-676.

Kempton, P.D., Fitton, J.G., Saunders, A.D., Nowell, G.M., Taylor, R.N., Hardarson, B.S. & Pearson, G., 2000, The Iceland plume in space and time: a Sr-Nd-Pb-Hf study of the North Atlantic rifted margin. *Earth and Planetary Science Letters* 177, 255-271.

Le Maitre, R.W., Bateman, P., Dudek, A., Keller, J., Lameyre, Le Bas, M.J., Sabine, P.A., Schmid, R., Sorensen, H., Streckeisen, A., Woolley, A.R., and Zanettin, B., 1989, *A Classification of Igneous Rocks and Glossary of Terms*. Blackwell, Oxford.

LaMeyre, J., Marot, A., Zimine, S., Cantagrel, J.M., Dosso, L., and Vidal, P., 1976, Chronological evolution of the Kerguelen Islands syenite-granite ring complex. *Nature* 263, 306–307.

Lassister, J.C. and Hauri, E.H., 1998, Osmium-isotope variations in Hawaiian lavas: evidence for recycled oceanic lithosphere in the Hawaiian plume. *Earth and Planetary Science Letters* 164, 483-496.

Mahoney, J.J., Macdougall, J.D., Lugmair, G. W., and Gopalan, K., 1983, Kerguelen hot spot source for Rajmahal Traps and Ninetyeast Ridge? *Nature* 303, 385-389.

Mahoney, J., Jones, W., Frey, F.A., Salters, V., Pyle, D. and Davies, H., 1995, Geochemical characteristics of lavas from Broken Ridge, the Naturaliste Plateau and Southernmost Kerguelen Plateau: Early volcanism of the Kerguelen hotspot, *Chem. Geol.*, 120, 315-345.

Mattielli, N., Weis, D., Blichert-Toft, J. & Albarede, F., 2002, Hf isotope evidence for a Miocene change in the Kerguelen Mantle plume composition. *Journal of Petrology* 43, 1327-1339.

Muller, R.D., Royer, J.-Y., & Lawver, L.A., 1993, Revised plate motions relative to the hotspots from combined Atlantic and Indian Ocean hotspot tracks. *Geology* 16, 275-278.

Nicolaysen, K., Frey, F.A., Hodges, K.V., Weis, D., & Giret, A., 2000, $^{40}\text{Ar}/^{39}\text{Ar}$ geochronology of flood basalts from the Kerguelen Archipelago, southern Indian Ocean: implications for Cenozoic eruption rates of the Kerguelen plume. *Earth and Planetary Science Letters* 174, 313-328.

Recq, M., Le Roy, I., Charvis, P., Goslin, J., & Brefort, D., 1994, Structure profonde du Mont Ross d'après la réfraction séismique (iles Kerguelen, Ocean Indien austral). *Canadian Journal of Earth Sciences* 31, 1806-1821.

Regelous, M., Hoffman, A.W., Abouchami, W. & Galer, S.J.G., 2003, Geochemistry of lavas from Emperor Seamounts, and the geochemical evolution of Hawaiian magmatism 85-42Ma. *Journal of Petrology* 44: 113-140.

Rhodes, J.M., 1996, Geochemical stratigraphy of lava flow samples by the Hawaiian Scientific Drilling project. *Journal of Geophysical Research* 101, 11729-11746.

Scoates, J.S., Lo Cascio, M., Weis, D., & Lindsley, D.H., 2006, Experimental constraints on the origin and evolution of the mildly alkalic basalts from the Kerguelen Archipelago, southeast Indian Ocean. *Contributions to Mineralogy and Petrology*, doi:10.1007/s004-006-0070-y.

Scoates, J.S., Weis, D., Franssens, M., Mattielli, N., Annell, H., Frey, F.A., Nicolaysen, K., Giret, A., 2007, The Val Gabbro plutonic suite: a sub-volcanic intrusion emplaced at the end of flood basalt volcanism on the Kerguelen Archipelago. *Journal of Petrology* 49, 79-105.

Storey, M., Saunders, A.D., Tarney, J., Gibson, I.L., Norry, M.J., Thirlwall, M.F., Leat, P., Thompson, R.N., & Menzies, M. A., 1989, Contamination of Indian Ocean asthenosphere by the Kerguelen–Heard mantle plume. *Nature* 338, 574 – 576.

Sun, S.-S., & McDonough, W.F., 1989, Chemical and isotopic systematics of oceanic basalts: implications for mantle composition and processes. In: Saunders, A.D., & Norry, M.J. (eds) *Magmatism in the ocean basins*. Geological Society, London, Special Publications 42, 313-345.

Tikku, A.A. & Cande, S.C., 2000, On the fit of Broken Ridge and Kerguelen Plateau. *Earth and Planetary Science Letters* 180, 117-132.

Wasserburg, G.J., Jacobsen, S.B., DePaolo, D.J., McCulloch, M.T., & Wen, T., 1981, Precise determination of Sm/Nd ratios, Sm and Nd isotopic abundances in standard solutions. *Geochimica et Cosmochimica Acta* 45, 2311-2323.

Weis, D. and Frey, F.A., Isotope geochemistry of Ninetyeast Ridge basement basalts: Sr, Nd and Pb evidence for the involvement of the Kerguelen Hotspot, Proceedings of the Ocean Drilling Program Leg 121, (eds., Weissel, J., Peirce, J. and Alt, J. et al.), pp. 591-610, 1991.

Weis, D., & Giret, A., 1994, Kerguelen Plutonic complexes: Sr, Nd, Pb Isotopic study and inferences about their sources, ages and geodynamic setting. Bulletin de la Société Géologique de France 166, 47-59.

Weis, D., Frey, F.A., Giret, A., and Cantagrel, J.M., 1998, Geochemical characteristics of the youngest volcano (Mount Ross) in the Kerguelen Archipelago: inferences for magma flux and composition of the Kerguelen plume. Journal of Petrology 39, 973-994.

Weis, D., Kieffer, B., Maerschalk, C., Pretorius, W., & Barling, J., 2005, High-precision Pb-Sr-Nd-Hf isotopic characterization of USGS BHVO-1 and BHVO-2 reference materials. Geochemistry Geophysics Geosystems 6, 10.1029/2004GC000852.

White, W.M., McBirney, A.R. & Duncan, R.A., 1993, Petrology and geochemistry of the Galapagos: portrait of a pathological mantle plum. Journal of Geophysical Research 98, 19533-19563.

Xu, G., F.A. Frey, D. Weis, J. Scoates, A. Giret, Flood basalts from Mt. Capitole in the central Kerguelen Archipelago: Insights into the growth of the archipelago and source components contributing to plume-related magmatism, Geochem Geophys. Geosyst., 8, Q06007, doi:10.1029/2007GC001608, 2007.

Yang, H.-J., Frey, F.A., Weis, D., Giret, A., Pyle, D. and Michon, G. , 1998, Petrogenesis of the flood basalts forming the northern Kerguelen Archipelago: Implications for the Kerguelen plume, Journal of Petrology, 39, 711-748.